IMPLEMENTATION OF THE SUPERSTRUCTURE/SUBSTRUCTURE JOINT DETAILS

Nebraska Department of Roads

Project Number SPR-PL-1(038) P514

Implementation of the Superstructure/Substructure Joint Details

NDOR Project Number SPR-PL-1(038) P514

FINAL REPORT

PRINCIPAL INVESTIGATOR

Maher K. Tadros

Charels J. Vranek Professor of Civil Engineering

University of Nebraska-Lincoln

December 2003

DISCLAIMER

The contents of this report reflect the views of the authors who are responsible for the facts and the accuracy of the data presented herein. The contents do not necessarily reflect the official views or policies of the Nebraska Department of Roads, nor the University of Nebraska-Lincoln. This report does not constitute a standard, specification, or regulation. Trade or manufacturers' names, which may appear in this report, are cited only because they are considered essential to the objectives of the report. The United States (U.S.) government and the State of Nebraska do not endorse products or manufacturers.

ABSTRACT

Prestressed concrete girder bridges are generally made continuous by adding longitudinal reinforcement in the deck over the pier. With this continuity method, the superstructure is continuous only for one-third of the total load. The pier diaphragm, which is normally cast prior to the deck, may experience distress because no negative moment resistance is available as the deck is being placed.

An innovative threaded rod continuity system was introduced to make the precast girders continuous for deck weight. Based on the connection detail developed in a previous NDOR project titled "Superstructure/Substructure Joint Details," a standard bolted connection detail was proposed to couple the precast girders. The precast girders are made continuous for approximately two-thirds of the loads, which results in reduced demand for prestress and for high strength concrete at release. The same girder size can span about 15 percent longer than the conventional system. Bridge performance is improved as the negative moment due to deck weight more than offset the positive moment due to time-dependent restraint without causing cracking at the piers.

The Clarks Viaduct is the first bridge in the United States to use the threaded rod continuity system. Its completion showed that this system is easy to construct without need for a specialty contractor. The system provides a feasible and cost-effective alternative for concrete superstructures to compete with long span steel bridges.

ACKNOWLEDGEMENTS

TABLE OF CONTENTS

LIST OF FIGURES

LIST OF TABLES

CHAPTER 1

INTRODUCTION

1.1   BACKGROUND

The use of precast prestressed girders in bridge construction started in the United States in the early 1950s. Since then, the use of pretensioned I-girders with cast-in-place (CIP) concrete decks has grown rapidly. Until the 1960s, bridges built with pretensioned I-girders and CIP concrete decks were designed as simply supported spans due to all dead loads and live loads. Although this type of construction provided simple design and construction procedures, it created a maintenance problem with deck joints over the piers. Leakage of deck joints, associated with the effects of deicing chemicals, has resulted in serious problems in the bearing devices and substructure of bridges. It is also aesthetically unappealing.

The potential for long-term maintenance costs associated with the deck joints and deck leakage over the substructure necessitates using continuity with precast prestressed girders. Current approaches to achieving such continuity include three methods: (1) adding longitudinal reinforcement in the deck slab, (2) post-tensioning by full length, and (3) coupling the top strands with extension. These methods are discussed below.

Method 1: Adding longitudinal reinforcement in the deck slab

In the early 1960s, many state agencies started to build continuous highway bridges with prestressed girders using this method. In this type of construction, the girder ends are embedded in cast-in-place diaphragms and the deck slab is made continuous without

1

any joints by adding longitudinal mild reinforcement in the deck slab over the pier. When the deck concrete cures and gains strength, additional loads from superimposed dead load and live load can be resisted by the continuous composite girder/deck section.

The prestressed girders are normally designed as simple beams due to their self-weight and deck weight, and as continuous beams due to superimposed loads. This method has become the conventional method for highway bridge construction. This method is the simplest and, possibly, the cheapest among the existing methods. It has served very well over the past three decades, especially in cold climate states where expansion joints over the piers create a maintenance problem.

However, the superstructure is continuous only for a small portion of the total load. If one assumes that the girder self-weight, the deck weight and the superimposed load each contribute approximately one-third to the total load, the system is actually continuous for only one-third of the total load. The relatively high pretension force, compared to that required in the other methods described below, causes creep growth of the member camber which is restrained by the pier diaphragms. The lack of permanent negative moment in that area may create a net positive restraint moment due to creep and cause bottom cracking at the piers. This "softening" of the negative moment region over the piers further reduces the continuity of the system.

Method 2: Post-tensioning by full length

Continuity is achieved through post-tensioning the full length of the bridge. Longitudinal post-tensioning provides higher resistance to stresses and allows longer spans for a given girder size than in Method 1. The structural design is optimized when

post-tensioning is partially introduced before deck placement. A second stage of post-tensioning after the deck has hardened helps prestress the deck and extend its life. However, it is the policy of the Nebraska Department of Roads (NDOR) and other state highway agencies to fully apply post-tensioning before the deck is placed. This is done to avoid calling in specialty post-tensioning contractors more than once and to guarantee that no special requirements are needed when the deck requires removal and replacement. This continuity method has been successfully used in highway bridges for many decades. It is an effective method, especially if spliced segmental I-beams are needed for spans longer than shipping capabilities of single-piece spans.

This method, however, requires anchorage blocks to resist stress concentrations at the anchorage zone. It also requires full-length ducts and usually necessitates widening of the beam web. In addition, a specialty contractor is often needed to perform the post-tensioning and grouting, which makes this method unattractive for many state agencies.

Method 3: Coupling the top strands with extension

This method creates continuity by coupling the top strands at adjacent member ends before the deck is cast. Without the post-tensioning duct and anchorage block, this method has the structural benefits offered by full-length post-tensioning. It was successfully used in the construction of a pedestrian bridge near Memorial Stadium in Lincoln, Nebraska.

The method of coupling girder top end strands involves in-field jacking of the strand ends to restore the prestress which existed before prestress release. It also requires a special coupling device. It is not feasible for use with highway bridges because a large

number of strands should be provided in the girder top flange to resist the negative bending moment.

Method 4: Coupling through high strength (H. S.) threaded rods

In 1998, University of Nebraska-Lincoln (UNL) researchers conceived the idea of coupling precast girders for deck weight using high strength threaded rods, as shown in Figure 1.1. It is referred to herein as a threaded rod continuity system. Girders are coupled using high strength threaded rods that are embedded in the girder top flange during fabrication. The threaded rods protrude beyond the girder ends and are coupled in the field at the diaphragms over the piers using the anchorage hardware with steel plates and heavy-duty nuts. The diaphragm concrete is then placed. When it gains adequate strength, deck placement begins. Full-scale testing of this system at the University of Nebraska, as illustrated in Figure 1.2, has shown that the precast girder with the high strength threaded rods had adequate strength and ductility. The experiments showed a superior behavior of this system in comparison with the conventional continuity system.

As opposed to Method 1, this method allows for the superstructure to be continuous for about two-thirds of the total load. The threaded rods are designed to resist the negative moment due to deck weight. After the deck concrete has hardened, reinforcing bars in the deck help resist the negative moments due to superimposed dead load and live load. Accordingly, this method can increase the span capacity of a given girder size by approximately 15% over Method 1. Unlike Method 1, this method creates a significant permanent negative moment that generally exceeds the positive restraint moment due to creep and eliminates any need for crack control bottom reinforcement over the piers.

1/2" Diameter bolts

Section A-A

2-2"x3"x26"
Steel bars

12"

1/2" Diameter bolt (Typ.)

1" Diameter, Grade 150 ksi
rod (Typ.)

3 1/2"

8 1/2"

A

A

10"

5"

3 1/2"

8 1/2"

Heavy nut
1 3/4" flat-to-flat
2" long (Typ.)

Plan View
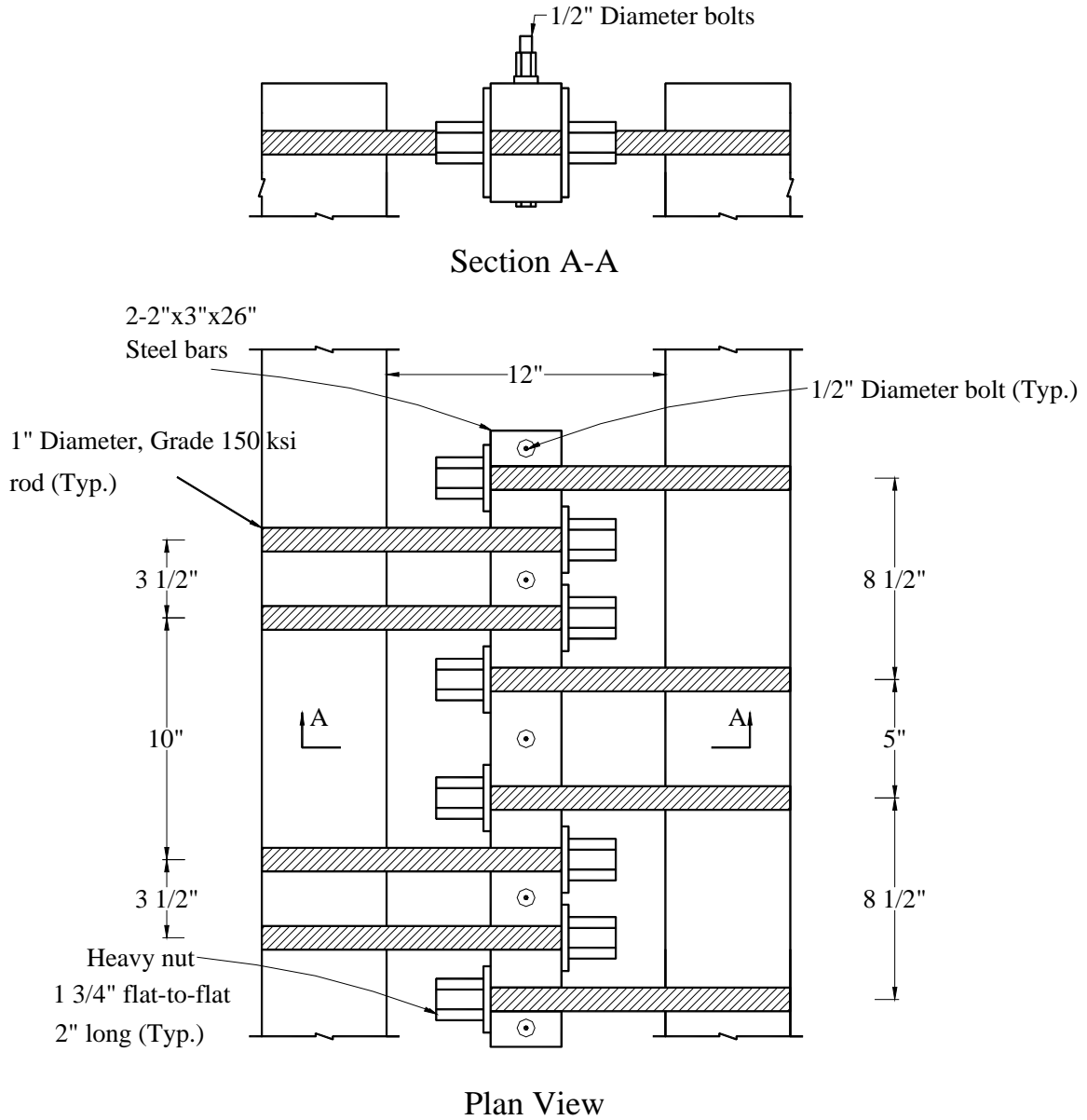
Figure 1.1 Threaded Rod Continuity Detail (Ma and Tadros, 1998)

5

Figure 1.2 Experimental Work by UNL in 1998

1.2 RESEARCH OBJECTIVES

The goal of this research is to implement the continuity detail, which has been developed in "SPR-PL-1(035) P514" project, in bridges in Nebraska. Based on an internal meeting of the NDOR bridge engineers and another meeting between NDOR bridge engineers and UNL researchers, NDOR agreed to implement the new detail for making the girders continuous for a bridge deck weight. This detail is expected to increase the span-to-depth ratio of the NU-Girders and it will be workable regardless the type of diaphragm used over pier locations (a continuous concrete diaphragm or steel diaphragm). Clarks Viaduct is assigned by NDOR to implement the new detail.

6

This project is also intended to present the investigation of the implementation bridges. The ultimate goal is that the system totally replaces the current inferior system of continuity in the deck for superimposed loads only. It is expected to be the standard system for precast concrete girder construction for Nebraska and the nation as well.

1.3 SCOPE AND LAYOUT

A total of five chapters are included in this report.

Chapter 2 introduces the optimized continuity details for coupling the precast girders based on the formerly experience in "SPR-PL-1(035) P514" research project. A standard bolt connection detail is proposed to be incorporated in the implementation bridge. Some considerations about the design of connection details are briefly discussed. Also presented in Chapter 2 are the advantages of the proposed system in comparison with the conventional continuity system based on a numerical example given in the PCI Bridge Design Manual.

In Chapter 3, the system analysis at both service limit state and ultimate limit state is discussed. Based on the nonlinear analysis at service limit state, the design criteria such as moment redistribution, crack control, and fatigue check of the threaded rod, are presented. The analysis is performed considering the precast and composite section over the negative moment zone. Flexural and shear strength design at ultimate are also included.

Chapter 4 discussed the system implementation. Three highway bridges including the Pflug Road Bridge, Clarks Viaduct, and Wood River Bridge, have been consequently

involved in implementation of the proposed continuity system. As the first implementation bridge in the United States, Clarks Viaduct, in Nebraska, is focused herein in terms of its design, construction, and monitoring.

Chapter 5 summarizes the conclusions of this research.

CHAPTER 2

SYSTEM DEVELOPMENT

2.1 OPTIMIZED CONNECTION DETAILS

This chapter presents the optimized continuity details for the threaded rod continuity system based on the work by UNL researchers in 1998. The continuity detail by Ma and Tadros was further modified to enhance the efficiency of the system during the prefabrication and construction process. The newly developed connection details are similar to those developed in 1998, except that the high strength threaded rods do not extend beyond girder ends and they are aligned in the longitudinal direction. Two connection details are presented: the welded connection detail and the bolted connection detail.

2.1.1 Welded Connection Detail

As shown in Figures 2.1, 2.2 and 2.3, a built-up steel box is used to couple each group of two threaded rods. The box is made of 50 ksi steel and E90 electrode is used for welding the plates. The longitudinal plates of the steel box are designed to carry a tensile force equivalent to the ultimate tensile force of two rods. The transverse plates are designed as a continuous beam supported by the longitudinal plates to resist bending and shear actions. The threaded rods are anchored with the steel box by heavy-duty nuts and washers. As shown in Figure 2.4, the rods are put in the girder top flange and they cover the negative moment zone to resist the moment due to deck weight.

9

The spacing of threaded rod is optimized as 6 in. to make the rods as close as possible to the I-girder web, thus protecting the thin girder top flange from breaking due to the pull-out force and guaranteeing enough cover for the threaded rods. Also, minimizing the spacing of threaded rods helps to reduce the bending moment of the transverse steel plate, which results in decreasing the plate thickness. The girder ends are produced with a 25 in.-long gap, which is large enough to place the steel box and couple the precast girders (see Figure 2.2). A demonstration specimen, shown in Figure 2.5, was produced by Rinker Materials, Inc., to verify the constructability of this welded connection detail.
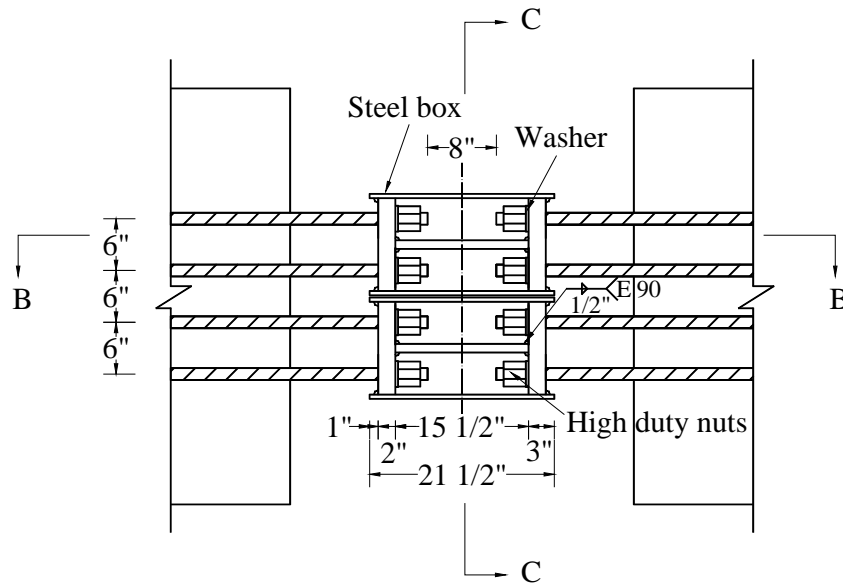
Figure 2.1 Welded Connection Detail Plan View: Section A-A

1 3/8" Diameter, Grade 150 ksi
threaded rod

Steel box

D

A

A

25"

25"

Pier centerline

D
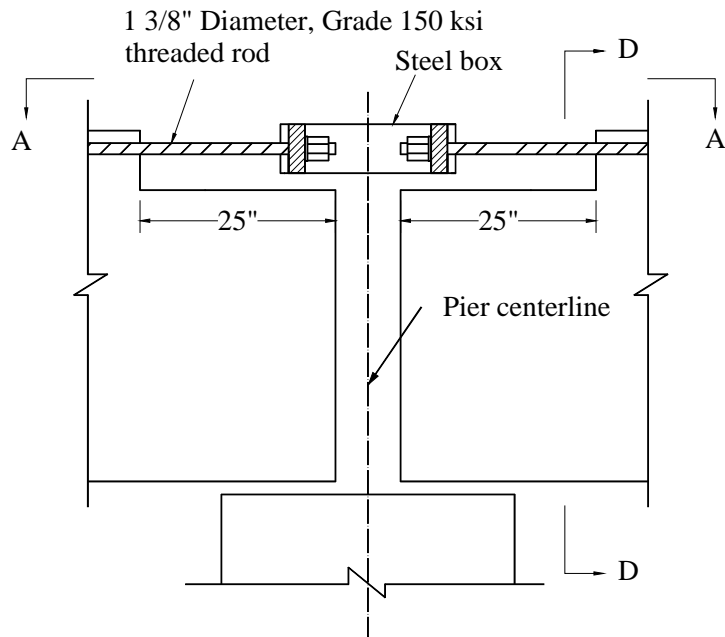
Figure 2.2 Welded Connection Detail: Section B-B

23 3/4"

4 7/8"

1"

4 7/8"

1/2"

1/2"

1/4"

1 1/2"

3"

6"

1 1/2"

3"

3"

7/8"

1"

1"

7/8"
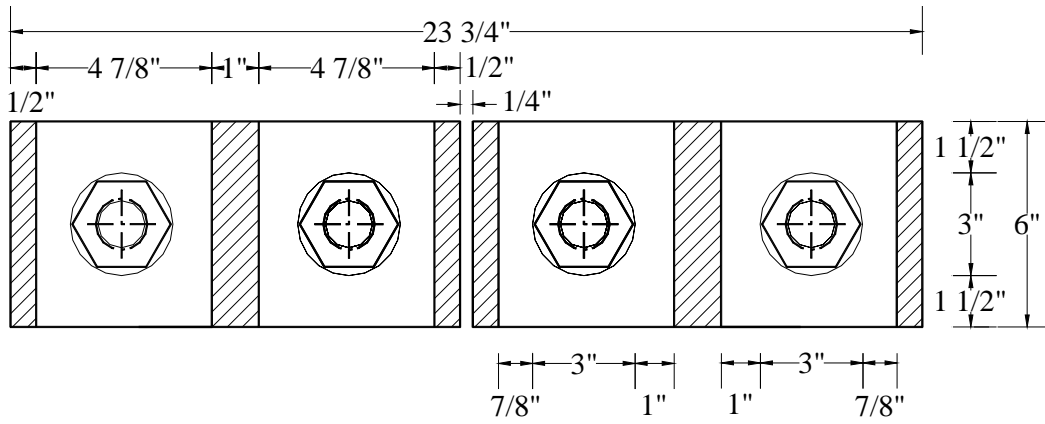
Figure 2.3 Welded Connection Detail: Section C-C
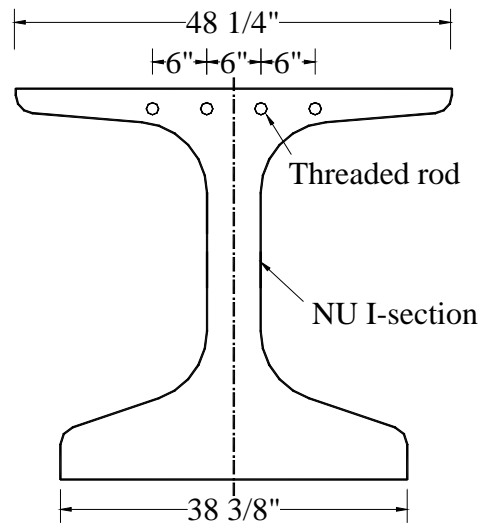
Figure 2.4 Precast Girder Section with Threaded Rods: Section D-D
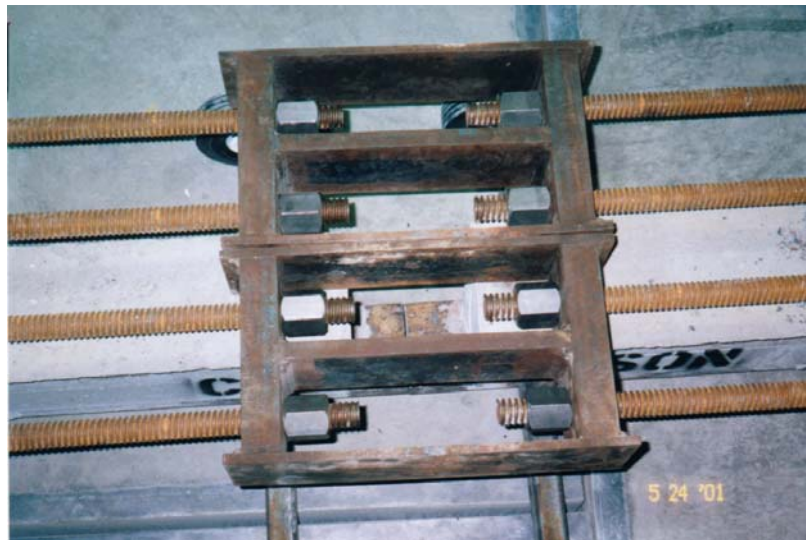
Figure 2.5 Welded Connection Detail Specimen

2.1.2 Bolted Connection Detail

As an alternative, the bolted connection detail was developed as shown in Figures 2.6, 2.7 and 2.8. Instead of using the welded steel boxes, the threaded rods are coupled by two Grade 50 ksi rectangular steel bars and five short Grade 150 ksi threaded rods. The

heavy-duty nuts and washers are also included in this connection detail to couple the rods with the rectangular steel bar. The rectangular steel bars are designed in bending and shear to support the ultimate tensile force of the four rods in the girder top flange.

A specimen was also made to demonstrate the bolted connection detail, as illustrated in Figure 2.9. This bolted connection detail was proposed since some bridge engineers might hesitate to use the welding connection detail due to concerns about potential fatigue problems.
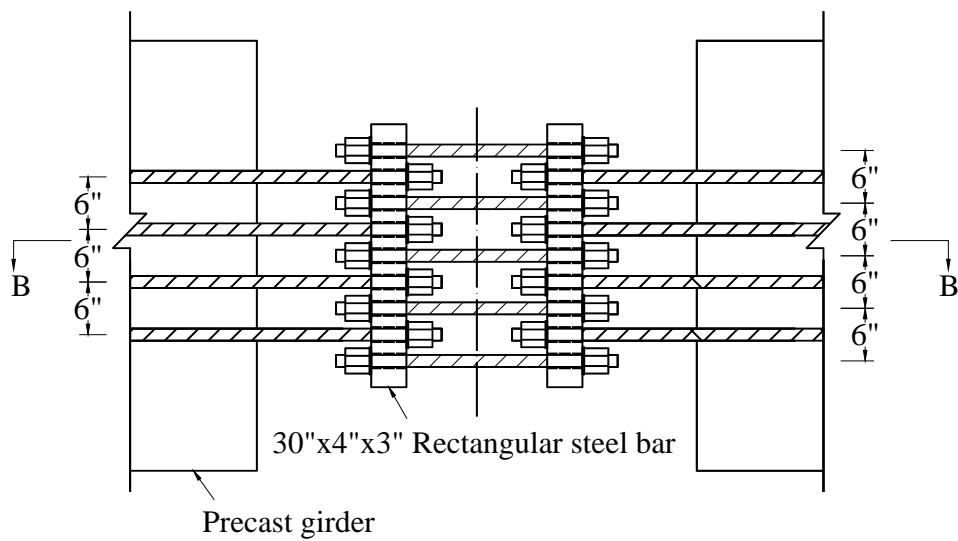
Figure 2.6 Bolted Connection Detail Plan View: Section A-A

1 3/8" Diameter, Grade 150 ksi threaded rod

Steel bar

A

A

25"

25"

$\mathrm{C_L}$ Pier
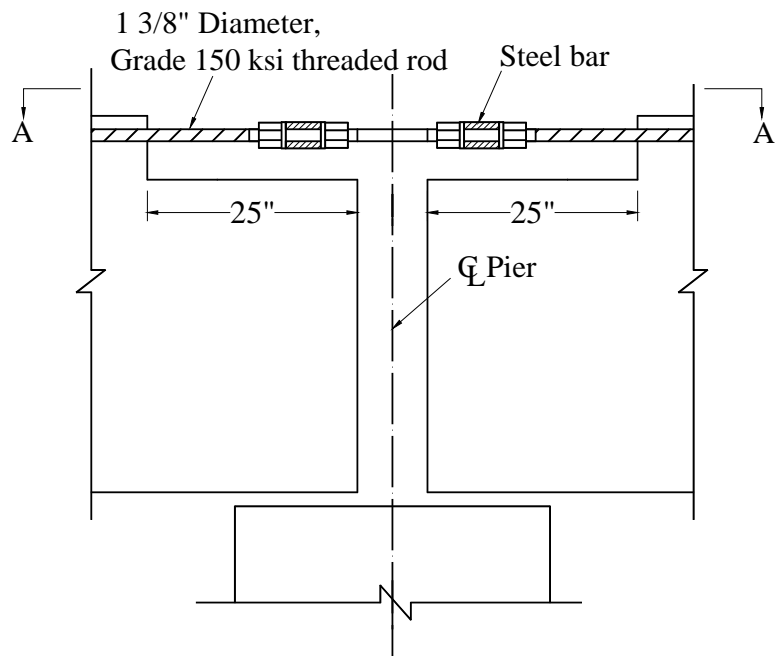
Figure 2.7 Bolted Connection Detail: Section B-B

3"
(Typ.)

3"
(Typ.)

3"

1 1/2"

30"
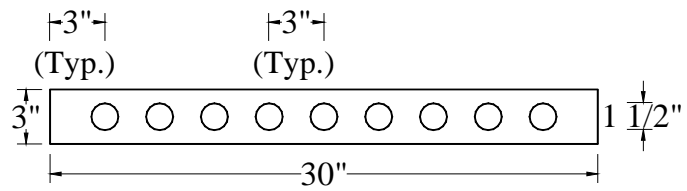
Figure 2.8 Rectangular Steel Bar Section

Figure 2.9 Bolted Connection Detail Specimen

14

Both the welded connection and bolted connection details can be easily used for construction. They cost about the same, which is $500. According to discussions with precast producers in Nebraska and Nebraska Department of Roads (NDOR) bridge engineers, the bolted connection detail was recommended as the standard to be used in the threaded rod continuity system.

2.2 DESIGN OF THE CONNECTION DETAILS

The steel box shown in Figure 2.1 and the rectangular steel rebar given in Figure 2.6 were designed assuming the maximum tensile capacity in the rod was evenly distributed over a length equal to the width of the nut plus the thickness of the washer. The shear force and bending moment diagram is conservatively obtained, assuming the threaded rods are unrestrained by the surrounding diaphragm concrete. Note that the rectangular steel rebar of 30"x4"x3", as shown in Figure 2.6, was designed based on the tensile capacity of 4-1 3/8 in. diameter, Grade 150 ksi threaded rods. If larger diameter threaded rods are used, the dimensions of the rectangular rebar may be increased accordingly.

2.3 ADVANTAGES OF THE PROPOSED CONTINUITY SYSTEM

The precast girders in the proposed continuity system are designed as simple span due to the girder self-weight, and continuous for the deck weight and superimposed loads. This system makes the superstructure continuous for about two-thirds of the total load. Since the maximum positive moment is greatly reduced in comparison with that of the conventional system, there is reduced demand for prestress and for high strength concrete

at release. With the same girder size, this system can increase the span capacity over 15% in comparison with the conventional system. Moreover, it creates a significant permanent negative moment that generally exceeds the positive restraint moment due to creep and eliminates any need for crack control bottom reinforcement over the piers.

To further illustrate the advantages of making precast girders continuous for deck slab weight, Example 9.6 of the PCI Bridge Design Manual is listed herein to make a comparison. The bridge given in this example has three spans, 110 ft + 120 ft + 110 ft, and is built with four Bulb Tees, BT-72, spaced at 12 ft. An interior girder supports the following loads: self-weight = 0.799 kips/ft, CIP deck slab weight = 1.222 kips/ft, superimposed dead load = 0.413 kips/ft, HL-93 LRFD Design Truck. Table 2.1 gives the service bending moment at two sections: 1) at 0.4L of the exterior span; and 2) at 0.5L of the interior span. The table provides the service bending moment for two cases: 1) the conventional system of making bridge continuous by adding longitudinal reinforcement in bridge deck, where no continuity is created for the deck slab weight; and 2) the proposed method where continuity is created before the deck slab is placed.

This table shows that creating continuity for the deck slab weight can reduce the service bending moment by 11 percent for the exterior span and by 26 percent for the interior span. These reductions result in a smaller amount of required prestressed force by about 20 percent. Thus, smaller girder size can be used and lower concrete strength at service and at release is required.

16

Table 2.1 Unfactored Bending Moment for the Conventional and Proposed Systems

Moment (ft-kips)	At 0.4L of exterior span		At 0.5L of interior span	
	Conventional system	Proposed system	Conventional system	Proposed system
Girder weight	1142.6	1142.6	1390.7	1390.7
CIP deck weight	1747.5	1129.8	2126.9	588.4
Barrier weight	139.0	139.0	73.0	73.0
Wearing surface weight	244.0	244.0	128.0	128.0
Live load	2382.9	2382.9	2115.0	2115.0
Total moment	5656.0	5038.3	5833.7	4295.2
Moment saving (%)	11%		26%	

CHAPTER 3

SYSTEM ANALYSIS

3.1 SYSTEM ANALYSIS AT SERVICE LIMIT STATE

A nonlinear analysis is performed to evaluate the threaded rod continuity system at service limit state. The analysis is presented in terms of moment redistribution, crack control, and fatigue limit check for the threaded rod. Moment redistribution is discussed herein and recommendations are provided to simplify the design using the proposed system. The flexural cracking control requirement is met by checking the spacing of the deck reinforcement at the top layer. The fatigue limit of the threaded rod is considered to satisfy the requirements in the AASHTO LRFD Bridge Design Specifications (LRFD Specifications).

Service limit state analysis is performed for both precast section and composite section at the negative moment area for multi-span bridge girders. The precast section is considered after the girders are coupled and at the time of deck placement, i.e., the deck weight is made continuous for the precast girder section. The composite section herein refers to that after the deck concrete hardens and the composite action occurs. A full load including the girder weight, deck weight, superimposed dead load and live load, are taken into account for the composite section.

The relationship between the moment applied to the girder section at the negative moment zone and the resulting curvature, from loading to failure, is presented to analyze

the system at service limit state. The analysis is conducted based on strain compatibility and force equilibrium. A few assumptions throughout the analysis are listed as follows:

1) Plain section remains plain after bending;

2) Stress-strain relationship for concrete is assumed as shown in Figure 3.1;

3) Stress-strain relationship for high strength threaded rod and low-relaxation strand are based on the power formula given by the PCI Bridge Design Manual. Figure 3.2 gives the stress-strain diagram for high strength threaded rod;
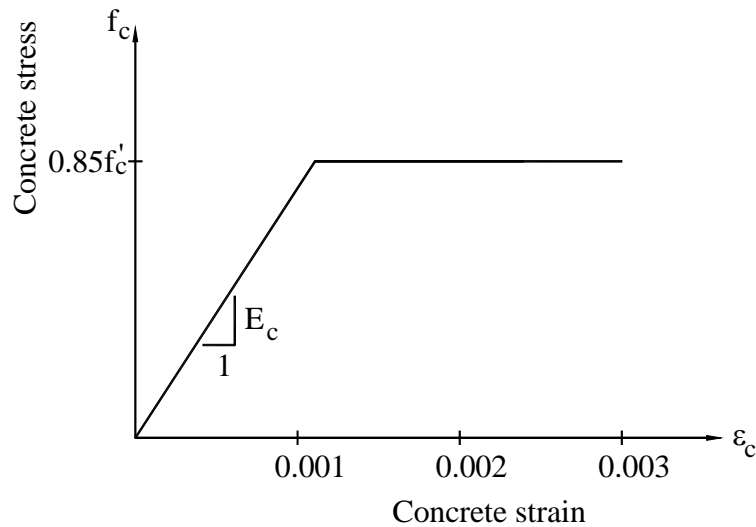
Figure 3.1 Stress-Strain Relationship of Concrete

The power formula is given as follows:

$$f_{si} = \varepsilon_{si} E_s \left[Q + \frac{1 - Q}{\left[1 + \left(\dfrac{\varepsilon_{si} E_s}{k f_y} \right)^R \right]^{1/R}} \right]$$

where: f_{si} is the steel stress; ε_{si} is the steel strain; E_s, Q, f_{py}, K, and R are parameters given in Table 3.1.
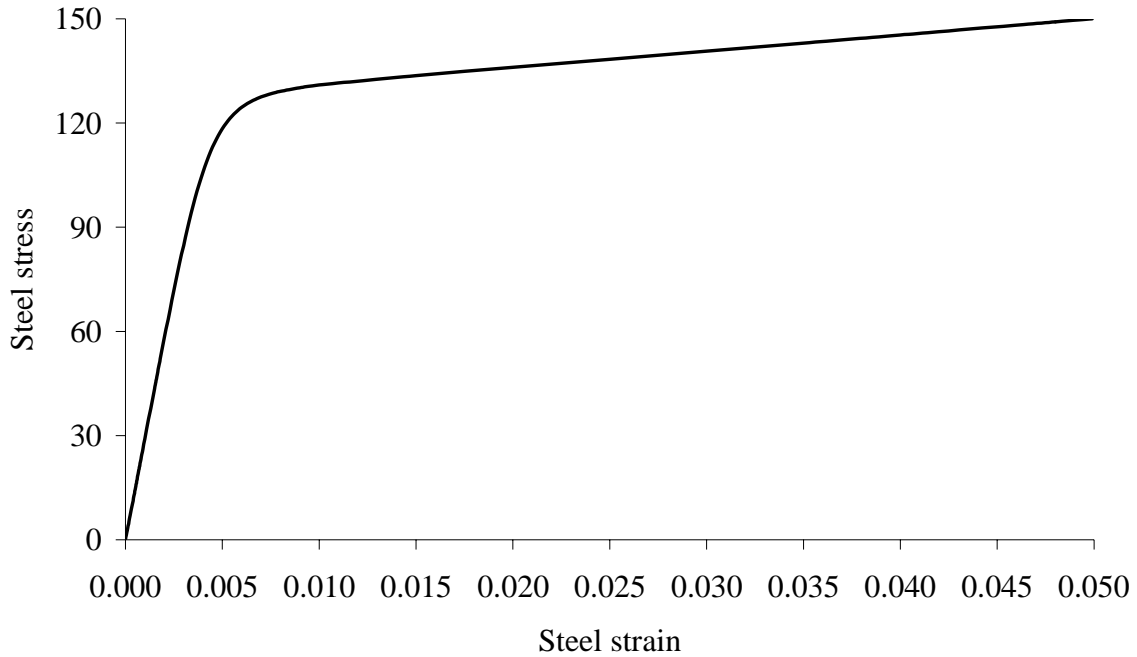
Figure 3.2 Stress-Strain Relationship of High Strength Threaded Rod

Table 3.1 Parameters in Power Formula for Threaded Rod and Strand

	Grade 150 threaded rod	Grade 270 strand
E_s	29000	28500
Q	0.016	0.031
f_{py}	127.5	243
K	1.01	1.04
R	4.99	7.36

To clarify the design criteria of the proposed system, a standard NU 1100 I-section girder with 7 in. CIP deck, shown in Figure 3.3-(a), is considered as an example of analysis. Concrete strength at 28 days, f'_c, is assumed as 8,500 psi for girder and 4,000 for deck. Effective flange width of the composite section is assumed to be 132 in. Five 1 1/2 in. diameter, Grade 150 ksi high strength threaded rods are embedded in the top flange of

20

the precast section over the negative moment zone. As Figure 3.3-(a) shows, the deck

reinforcement is #5@12 in. at the bottom layer and (#4 + 2#7) @ 12 in. at the top layer. It

is assumed that the distances from the center of steel to the concrete bottom fiber are

41.08 in. for threaded rods, 45.24 in. for deck rebar at the bottom layer, and 47.40 in. for

deck rebar at the top layer, respectively.
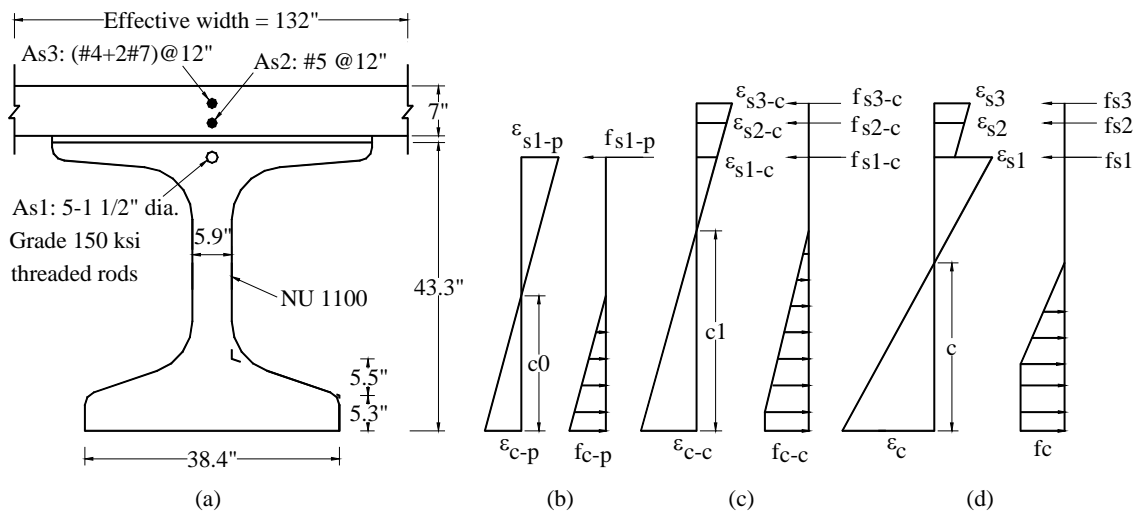
Figure 3.3-(a) Bridge section with reinforcement for analysis; (b) Strain and stress diagram of precast section due to deck weight; (c) Strain and stress diagram of composite section due to superimposed dead load and live load; (d) Final strain and stress diagram.

Figure 3.3-(b) illustrates the strain and stress diagrams of the precast section subject

to the negative moment due to deck weight. The strain and stress diagrams of composite

section due to superimposed dead load and live load are given in Figure 3.3-(c). Note that

the uncracked precast section and deck section are not shown for clarity, but they are

included in the analysis. Tensile strain of concrete for a cracked section is ignored. It is

further assumed that tension cracks have progressed all the way to the neutral axis. The

strain diagrams in Figure 3.3-(b) and Figure 3.3-(c) are superimposed to obtain the final

strain diagram as shown in Figure 3.3-(d), where a final neutral axis location is presented.

The stress diagrams of precast section and composite section are shown corresponding to the strain diagrams.

Based on Figure 3.3-(d), the strain compatibility and force equilibrium are maintained. An Excel spreadsheet program was developed to perform the analysis. For a given section, the program considered a gradually increased loading which corresponds to a concrete compressive strain at the bottom fiber varying from zero to the ultimate strain of 0.003. At each concrete compressive strain, the neutral axis, c, is obtained through an iterative process to satisfy the strain compatibility and force equilibrium. The process is iterative due to the nonlinearity of the stress-strain relationship of the concrete and steel. Once the neutral axis, c, is obtained, the curvature of the section, φ, is computed by

$$\varphi = \frac{\varepsilon_c}{c}.$$

The moment-curvature diagrams are plotted for both the precast and composite sections. Shown in Figure 3.4 are three curves, which respectively represent the moment-curvature relationship for the precast girder section just after deck placement, precast section after deck concrete is hardened, i.e., composite section, and deck section. The diagram of deck section is parallel to that of the composite section since an initial curvature of the precast section occurs due to deck weight prior to the formation of composite action. The maximum flexural moment at service limit state is shown as 4141 ft-kips for the given section. This value is obtained by dividing the ultimate flexural strength of the composite section by a factor of 1.75. Similarly, the maximum unfactored moment due to deck weight and operation loading during deck placement is determined

to be 2145 ft-kips. This factor of 1.75 is assumed for simplicity. The maximum moment at service limit state is presented to show that both the precast and composite sections under the service loading behave elastically, or very nearly so.
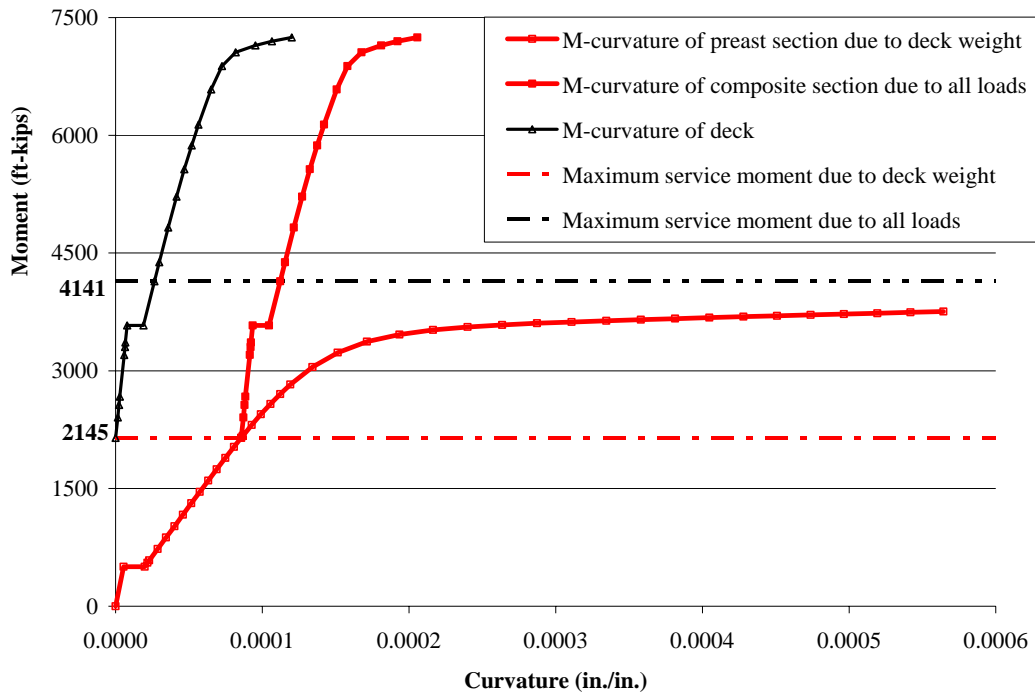
Figure 3.4 Moment-Curvature Relationship of the Analyzed Section over Pier

The section at the negative moment zone is actually a conventionally reinforced section, where cracking normally occurs at the service limit state. While the pretensioned section at the positive moment area is non-cracked, the moment redistribution due to the reduced section at the negative moment zone needs to be included in the analysis.

Based on the classical elastic equation, the curvature of a section can be expressed in terms of bending moment and flexural rigidity as follows: $\varphi = \dfrac{M}{EI}$, that is, $I = \dfrac{M}{E\varphi}$.

Thus, the moment of inertia of the uncracked precast section is determined as 197904 in.[4], which can be alternatively obtained from the transformed section consisting of

concrete only by replacing the threaded rods with an equivalent concrete area. The cracking moment, M_{cr}, is 503 ft-kips. The moment of inertia of the cracked precast section subject to the moment at service limit state, assumed within the range between 503 ft-kips and 2145 ft-kips, can be computed to be 54614 in.[4]. As shown in Figure 3.4, the composite section is assumed to be formed at the maximum service limit state moment due to deck weight, noted as $M_0 = 2145$ ft-kips. The curvature subject to M_0, is $\varphi_0 = 0.0000856$ for the precast section, which is also the initial curvature of the composite section. To obtain the moment of inertia of the composite section,

$$I = \frac{(M - M_0)}{E(\varphi - \varphi_0)}$$ is used, where the initial values of φ_0 and M_0 are deducted. Accordingly,

the moment of inertia is determined as 391476 in.[4] for the uncracked composite section (before deck concrete at the top fiber cracks), and 161742 in.[4] for the cracked composite section, respectively.
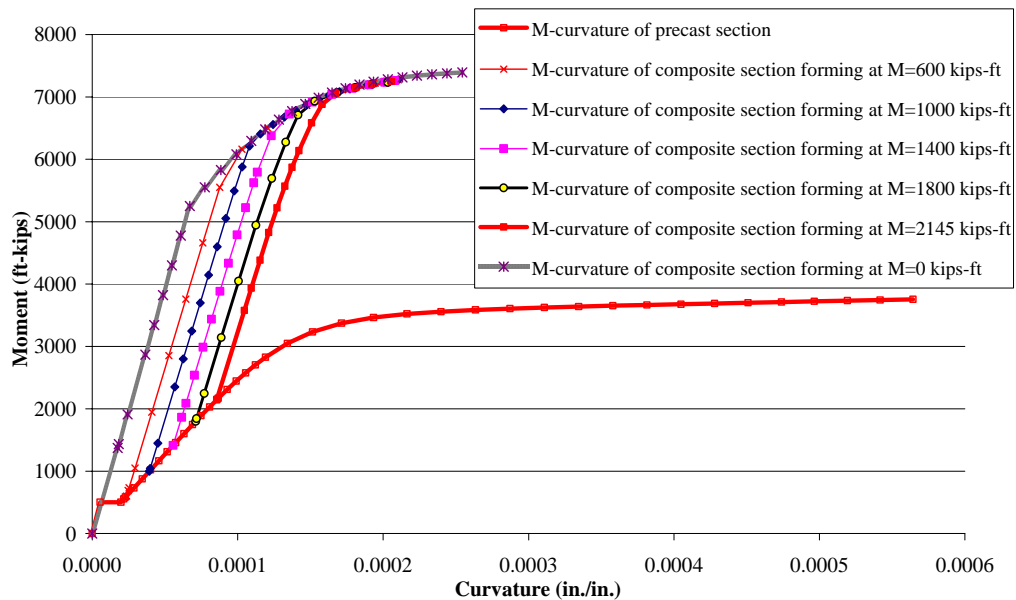
Figure 3.5 Moment-Curvature Diagrams Considering Composite Section Formation at Various Moment due to Deck Weight

Figure 3.5 shows several moment-curvature diagrams of the composite section formed at different moments due to deck weight. Note that the composite section before deck concrete in tension cracks is not shown for clarity. The moment-curvature diagram of the deck section is not shown since only the composite section is focused herein. It is shown that all diagrams of the composite section, except that formed at $M = 0$, are parallel to each other within the elastic stage. Figure 3.5 is plotted to show that the moment of inertia of a composite section is independent of the applied moment due to deck weight as long as the section maintains the elastic behavior. The diagram of the composite section forming at $M = 0$ is presented for comparison purposes only. It is plotted without considering the initial strain of concrete and threaded rod at the precast section before the formation of composite section, which is currently an acceptable way to perform the analysis. It normally ends up with a little higher ultimate flexural strength compared with those shown in Figure 3.5 considering the initial strain. However, it may result in significant errors in analyzing the steel stress at service limit state, which will be described shortly in the chapter.

To investigate the impact of the amount of deck reinforcement on the moment of inertia at the cracked composite section, Figure 3.6 is presented considering various composite sections with different amount of deck reinforcement. The precast section shown in Figure 3.3 (a) was used and kept the same for all cases. In terms of deck reinforcement in the composite section, #5 rebar @12 in. as the bottom layer is assumed for all cases. The amount of deck reinforcement at the top layer, A_{s3}, varies from 0 to 20 in.^{2} with an interval of 2. Note that the composite sections before the deck concrete in

tension cracks are not shown for clarity. Provided that the composite section is subject to the moment at service limit state, the larger the amount of deck reinforcement, the larger slope of moment-curvature diagram is obtained, which indicates the larger I_{cr} value.
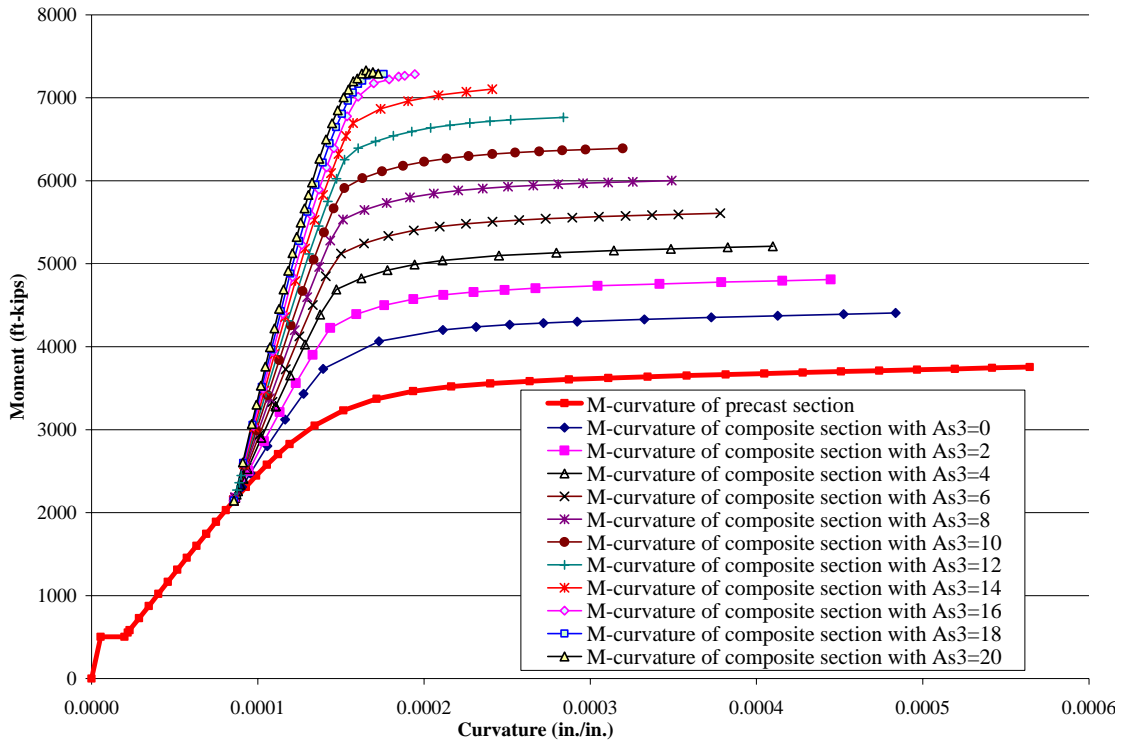
Figure 3.6 Moment-Curvature Diagrams of Composite Section with Fixed Amount of Threaded Rods and Various Amount of Deck Reinforcement

Figure 3.7 is provided to investigate the impact of the amount of threaded rod on the moment of inertia for the cracked composite section. Seven sets of sections are included, which are reinforced with various amount of threaded rod in the precast section, but with the same amount of deck reinforcement. Note that "i-p" (i= 1, 2, …7) refers to the ith case of the precast section. The amount of threaded rod in the precast section is respectively 0, 1.25, 1.70, 3.16, 4.74, 6.32, and 8.50 in.^{2} corresponding to case i (i = 1, 2, …7). No graph is shown for the case 1-p since no curvature occurs in this special case, where no continuity is made for deck weight. Similarly, "i-c" represents the ith case of composite

26

section, which is assumed to be formed at the maximum service moment due to deck weight for each case considered. The deck reinforcement is same for all cases, which is #5@12 in. at the bottom layer and (#4+2#7)@12 in. at the top layer. As shown in Figure 3.7, the larger the amount of threaded rod in the precast section, the larger the I_{cr} value obtained for the composite section. Note that the composite section before the deck concrete at top fiber cracks is not included for clarity. In the case "2-c" where the amount of threaded rod is very small, the I_{cr} value of the composite section is very close to that of case "1-c", where no threaded rod is included. The I_{cr} value based on the moment-curvature diagrams is used to analyze the moment redistribution for the threaded rod continuity system.

Note: i-p (i=1, 2, .., 7) represents the precast section; i-c represents the composite section.
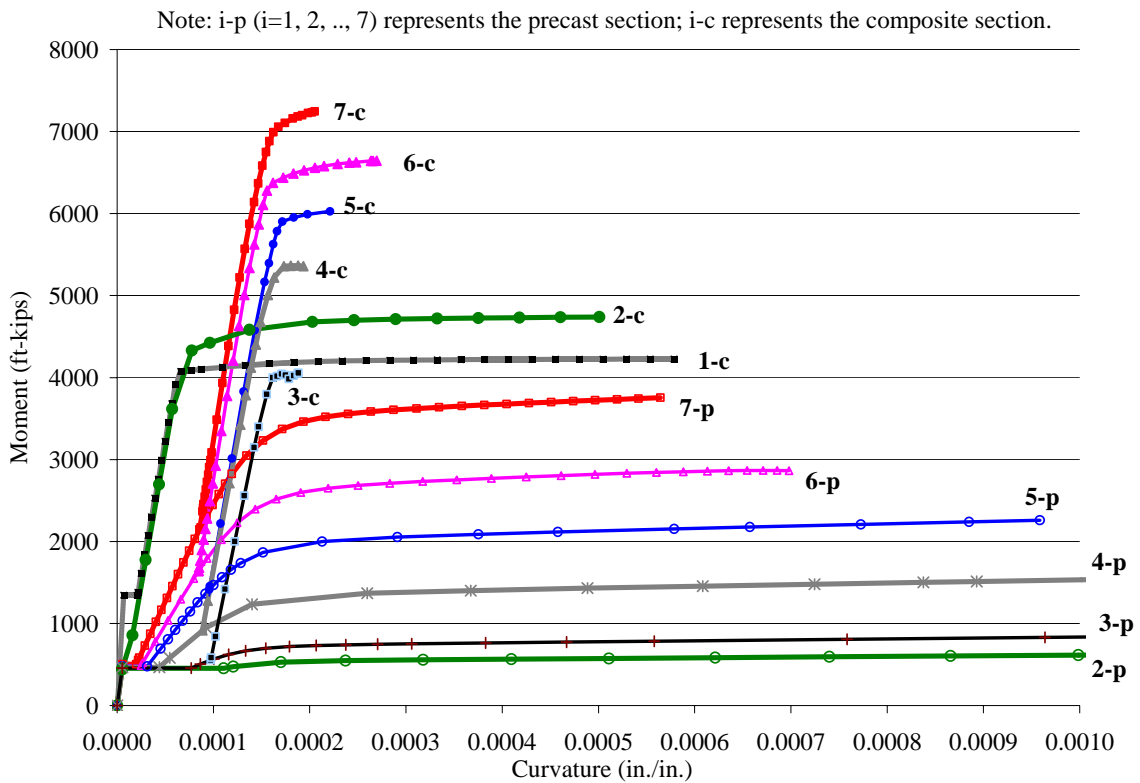
Figure 3.7 Moment-Curvature Diagrams for Sections with Various Amount of Threaded Rod and Fixed Amount of Deck Reinforcement

27

3.1.1 Moment Redistribution

An iteration process is required to determine the moment redistribution due to deck weight on the precast section and all loads on the composite section. The negative moment zone is divided into eight segments to account for the effective moment of inertia at various locations. The empirical expression of effective moment of inertia, I_e, by Branson is shown as follows:

$$I_e = \left(\frac{M_{cr}}{M_a}\right)^m I_g + \left[1 - \left(\frac{M_{cr}}{M_a}\right)^m\right] I_{cr} \text{ and } I_e \leq I_g$$

where I_{cr} is the moment of inertia of a cracked section, which can be obtained from the moment-curvature diagram as discussed above. The power $m = 4$ is used for determination of I_e in an individual section.

A two-span bridge of 100 ft + 100 ft using a standard NU 1100 I-section girder was considered to investigate the moment redistribution due to deck weight. It is assumed the girder weight is 0.724 kips/ft and deck weight is 1.132 kips/ft. Also assumed is 5 in.[2] threaded rod in the precast section. Based on the elastic theory, the moment due to girder weight plus deck weight is used to start the iteration process of determining the effective moment of inertia, I_e, at each segment. The continuous span with various I_e values at the negative moment zone and full section at the positive moment area is then analyzed due to deck weight, which results in a moment redistribution. Based on the redistributed moment, new I_e values are obtained. The iteration process is continued until the moments from the adjacent steps differ within a 5 percent range.

Table 3.2 gives the results at each iteration step. Note that M5 to M8 refer to the four segments at the negative moment zone between the 0.9span and the centerline of pier. M1 to M4 represent the segments between the 0.8span and 0.9span, which are not shown in the table for clarity. The moment of inertia of NU 1100 I-section, I_{girder} = 182279 in.^{4} is put to start the iteration. Based on this constant section along the span, the moment at M8 is -1415 ft-kips. After several iteration steps, the negative moment at M8 due to deck weight converges approximately at -1072 ft-kips, which is 75.7% of -1415 ft-kips as the started moment value. Thus, 24.3% of the negative moment is redistributed.

Table 3.2 Analyzing Moment Redistribution due to Deck Weight by Iteration

		Negative moment sections at 0.9span to centerline of pier			
		M5	M6	M7	M8
Starting	I girder	182279	182279	182279	182279
	Moment	-916	-1075	-1242	**-1415**
1 Iteration	Ie	118111	54326	40637	36520
	Moment	-444	-590	-744	-904
2 Iteration	Ie	182279	182279	127817	54793
	Moment	-712	-866	-1027	-1195
3 Iteration	Ie	182279	103925	51265	39690
	Moment	-531	-680	-836	-999
4 Iteration	Ie	182279	182279	83938	47089
	Moment	-644	-796	-955	-1121
5 Iteration	Ie	182279	150980	59046	41678
	Moment	-573	-723	-880	-1044
6 Iteration	Ie	182279	182279	72073	44649
	Moment	-617	-768	-926	-1091
7 Iteration	Ie	182279	180073	63270	42683
	Moment	-592	-743	-900	-1065
8 Iteration	Ie	182279	182279	67871	43730
	Moment	-606	-757	-915	-1080
9 Iteration	Ie	182279	182279	65224	43133
	Moment	-598	-749	-907	**-1072**

Note: Moment of inertia is in in.^{4} and moment in ft-kips.

Various amounts of threaded rod in the precast section are considered to account for its impact on the moment redistribution due to deck weight. Based on the ultimate state limit analysis, 5 in.^{2} is the required amount of threaded rod to resist the moment due to

deck weight, which is referred herein to $A_{s1\ required} = 5$ regarding this span case of 100 ft + 100 ft. If 6 in.[2] threaded rod is provided in the precast section, that is, the ratio of $A_{s1}/A_{s1\ required} = 6/5 = 1.2$, 22.2 percent of moment redistribution is similarly obtained. Accordingly, the theoretical data is shown in Fig. 3.8 as a point (1.2, 22.2%). For the span case of 100 ft + 100 ft, the moment redistribution varies approximately from 19% to 24% corresponding to the ratio of $A_{s1}/A_{s1\ required}$ from 1.0 to 1.6. Note that other span cases, 110 ft +110 ft, 120 ft + 120 ft, and 130 ft + 130 ft, are included in the figure. It shows an approximate range of 18% to 26% negative moment to be redistributed.
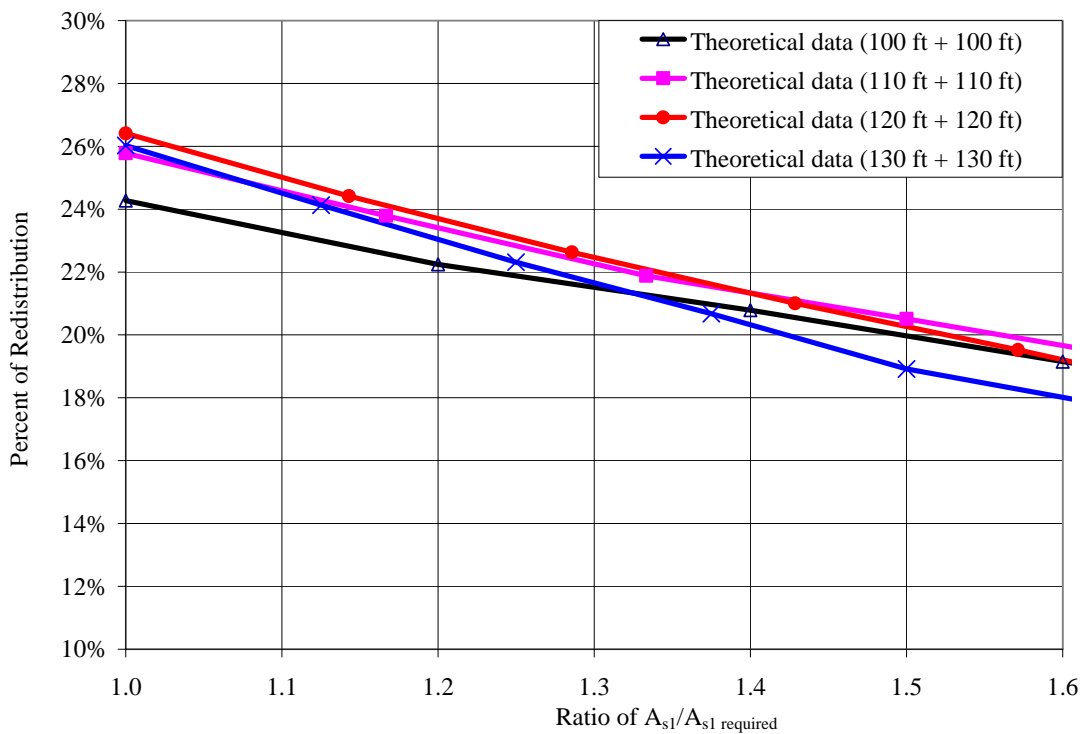
Figure 3.8 Theoretical Data of Moment Redistribution due to Deck Weight

Figure 3.9 illustrates the moment redistribution of the theoretical data and those based on the ACI 318-02 Building Code (ACI 02 Code) and the AASHTO LRFD Bridge Design Specifications (LRFD Specifications). Note that only two span cases of 100 ft +100 ft and 130 ft +130 ft are shown for clarity. According to the ACI 02 Code, Art. 8.4,

the negative moment shall be permitted to increase or decrease that from elastic theory by $1000\varepsilon_t$, with a maximum of 20 percent, provided that ε_t is equal to or greater than 0.0075 at the section at which moment is reduced. ε_t is defined as the net tensile strain in extreme tension steel at nominal strength. The LRFD Specifications state that negative moments determined by elastic theory at strength limit states may be increased or decreased by not more than the following percentage: $20\left(1 - 2.36\dfrac{c}{d_e}\right)$.

The negative moment redistribution results in increasing the positive moment for service limit state design. To obtain a conservative design, no reduction is recommended for the negative moment zone design, but the increase of positive moment due to moment redistribution is taken into account. Note that a range of 18% to 26% negative moment redistribution approximately corresponds to 7% (7% = 18% x 0.4) to 10% (10% = 26% x 0.4) increase of positive moment at 0.4span section considering a two-span bridge. Figure 3.10 shows the theoretical data of the positive moment increase as well as those based on the ACI 02 Code and the LRFD Specifications. Note that the theoretical increase of positive moment varies approximately between 10% and 7%, which changes very little. Similarly, the range between 12% and 8% can be obtained considering the case of a multi-span bridge. Thus, 12% can be simply used in the actual design to account for the increase of positive moment due to moment redistribution for deck weight, which increases the required prestress force for service limit state design. For example, if the negative moment due to deck weight is determined as 1415 ft-kips, the increase of positive moment due to moment redistribution is $12\%(1415) = 170$ ft-kips.
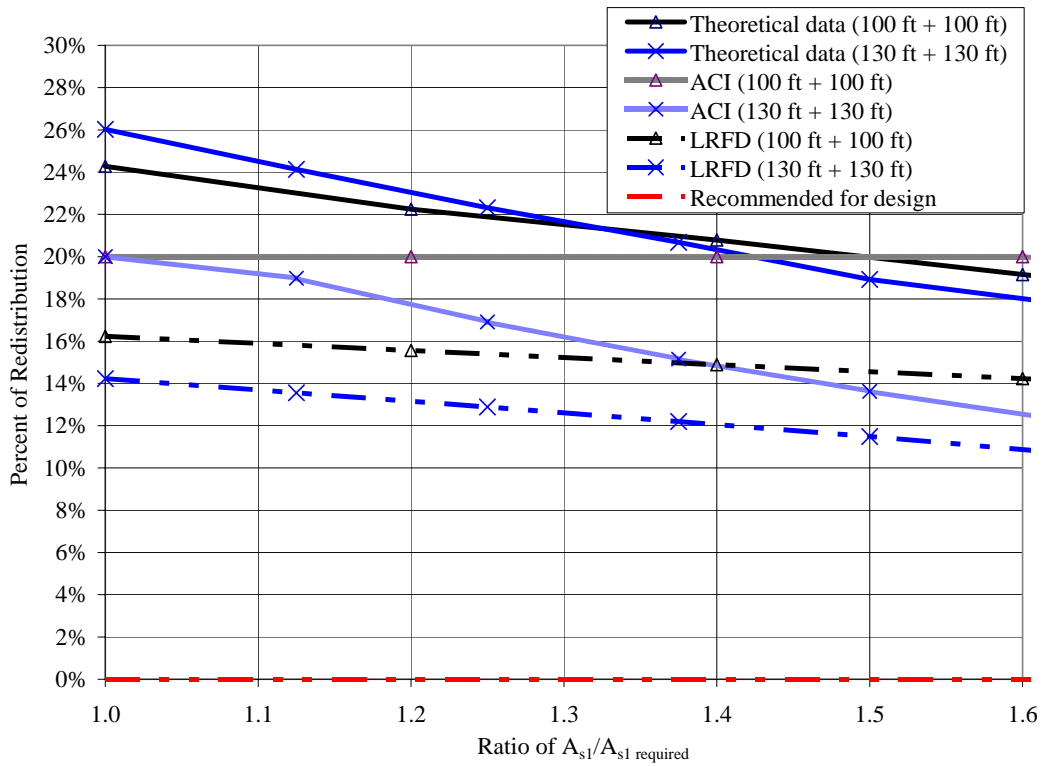
Figure 3.9 Comparison of Moment Redistribution due to Deck Weight
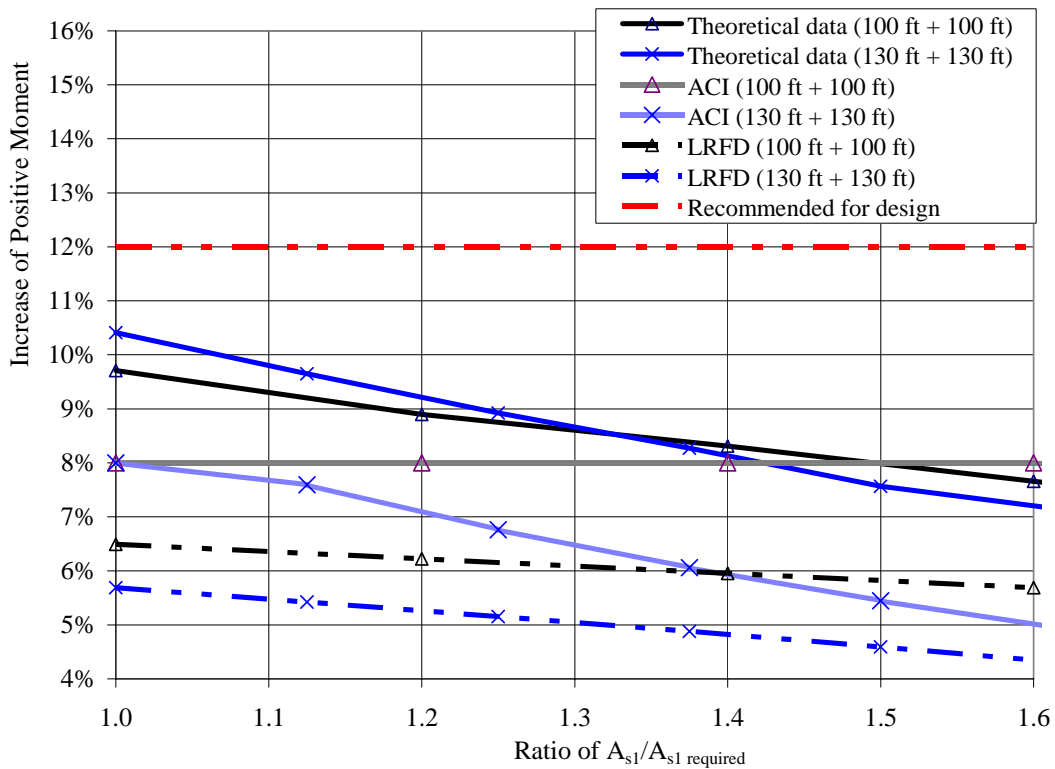
Figure 3.10 Increase of Positive Moment due to Moment Redistribution

32

A similar analysis was performed for the composite section due to all loads. It was found that the positive moment was marginally impacted, so the details are not shown herein.

3.1.2 Crack Control

According to the LRFD Specifications, the following formula for crack control is used:

$$f_{sa} = \frac{Z}{(d_c A)^{1/3}} \leq 0.6 f_y$$

Setting A =$2d_c$s,

$$f_{sa} = \frac{Z}{(2d_c^2 s)^{1/3}} \leq 0.6 f_y$$

Thus, $s = \dfrac{Z^3}{2 f_{sa}^3 d_c^2}$ and $f_{sa} \leq 0.6 f_y$

The spacing of deck reinforcement at the top layer over the negative moment area can be determined to control the cracking. Figure 3.11 shows the moment-steel stress diagram of the threaded rod and that of the top layer deck rebar based on the section given in Figure 3.3. The deck section before cracking is considered. Assume that the composite section forms with the deck weight moment of 2145 ft-kips. Any loading moment higher than this value is carried by the composite section. When the maximum moment is 4141 ft-kips for the composite section at service limit state, the stress of the top layer deck reinforcement can be determined from the figure as 23.5 ksi. Accordingly, the spacing of

rebar, $s = \dfrac{Z^3}{2 f_{sa}^3 d_c^2} = \dfrac{120^3}{2(23.5)^3 2^2} = 16.6$ in., where Z = 130 kips/in in severe exposure

condition is assumed.
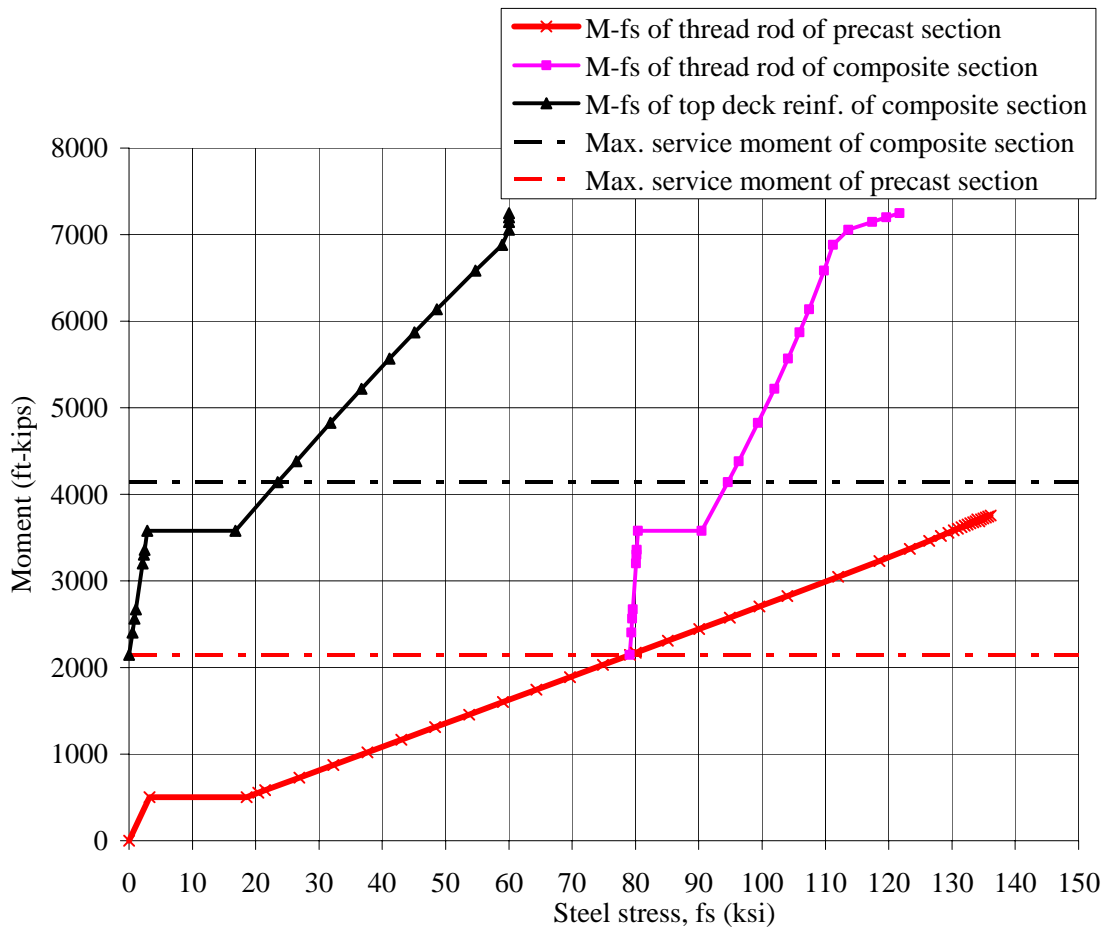
Figure 3.11 Moment-steel Stress Diagram of the Threaded Rod and Top Layer Deck Reinforcement

Based on a review of past research, parametric studies comparing various crack width

predictive methods, and results from actual design example problems, an equation similar

to the Frosch cracking model adopted by the ACI 318 is proposed for consideration by

AASHTO (see Reference by Destefano and Tadros). The proposed AASHTO equation is

as follows:

34

$$f_{sa} = \frac{700\gamma_e\gamma_r}{\beta(s+2d_c)} \le 0.8f_y$$

where,

f_{sa} = allowable service level stress in the reinforcement, ksi;

γ_e = exposure factor,

= 1.0 for Case 1, which is moderate exposure condition,

= 0.75 for Case 2, which is severe exposure condition;

γ_r = reinforcement factor,

= 0.75 for smooth weld-wire fabric,

= 1.00 for all other types of reinforcement;

β = $1 + \dfrac{d_c}{0.7(h-d_c)}$;

The formula can be expressed in form of steel spacing as follows:

$$s = \frac{700\gamma_e\gamma_r}{\beta f_{sa}} - 2d_c \text{ and } f_{sa} \le 0.8f_y$$

In the example considered herein, f_{sa} is determined as 23.5 ksi $\le 0.8f_y = 48$ ksi.

Assume $\beta = 1 + \dfrac{d_c}{0.7(h-d_c)} = 1 + \dfrac{2.31}{0.7(50.3-2.31)} = 1.07$, then

$$s = \frac{700(1)(1)}{1.07(23.5)} - 2(2.31) = 23.2 \text{ in.}$$

The deck top reinforcement is (#4+2#7)@12 in., which provides a smaller spacing than that required by both the LRFD Specifications and the proposed formula, thus the control of cracking can be satisfied. Note that the deck reinforcement is normally spaced

less than 12 in. at the negative moment zone based on the ultimate strength design, which

indicates that crack control criterion can mostly be guaranteed.
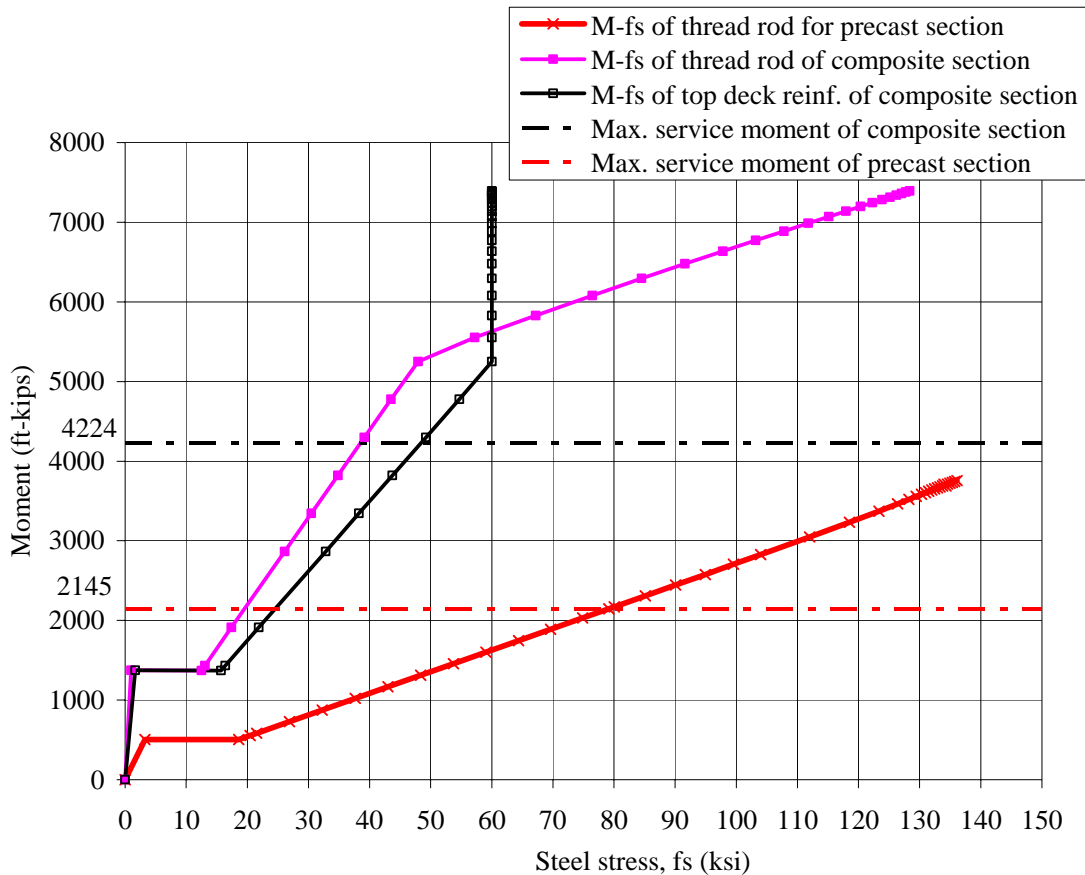
Figure 3.12 Moment-Steel Stress Diagram of the Threaded Rod and Top Layer Deck
Reinforcement without Considering the Initial Strain due to Deck Weight

The composite section over the pier might be normally analyzed without considering

the initial strain of concrete and threaded rod due to deck weight prior to the formation of

the composite section. But this analysis results in some errors, which can be seen by

comparing Figure 3.12 with Figure 3.11. In Figure 3.12, the analysis is performed for the

precast section and composite section separately, which indicates that no initial strain is

included in the composite section analysis. Instead of a value of 23.5 ksi given in Figure

36

3.11, Figure 3.12 shows that the stress of the top layer deck rebar is approximately 49 ksi subject to the maximum service limit state moment. Also, it predicts a more ductile composite section than it should be. The stress of the threaded rod in the composite section seems more misleading. Consider the stress of the threaded rod subject to the maximum service moment due to deck weight, shown as 2145 kip-ft. According to Figure 3.12, the rod stress of the precast section is about 80 ksi but is only about 20 ksi of the composite section. This obviously underestimates the stress of the threaded rod. As a comparison, Figure 3.11 shows a value of 95 ksi for the rod stress. Therefore, the initial concrete and threaded rod strain due to the intermediate loading stage of deck weight should be considered in the analysis.

3.1.3 Fatigue Check

When consideration of fatigue is required, the stress range is determined using the fatigue load combination as specified in the LRFD Bridge Design Specifications. The stress range in straight reinforcement resulting from the fatigue load combination shall not exceed:

$$f_f = 21 - 0.33 f_{min} + 8\left(\frac{r}{h}\right)$$

Assuming $f_{min} = 0$ and $\frac{r}{h} = 0.3$, $f_f = 21 - 0.33(0) + 8(0.3) = 23.1$ ksi.

The stress range in prestressing tendons shall not exceed 18.0 ksi for radii of curvature in excess of 30.0 ft. Since no fatigue stress limit is specified in the LRFD Bridge Design Specifications for the threaded rod, the smaller limit of reinforcement and

strands, which is 18.0 ksi, is conservatively used. The stress of the threaded rod due to live load at fatigue limit state is obtained from Figure 3.13 to check the fatigue criterion.
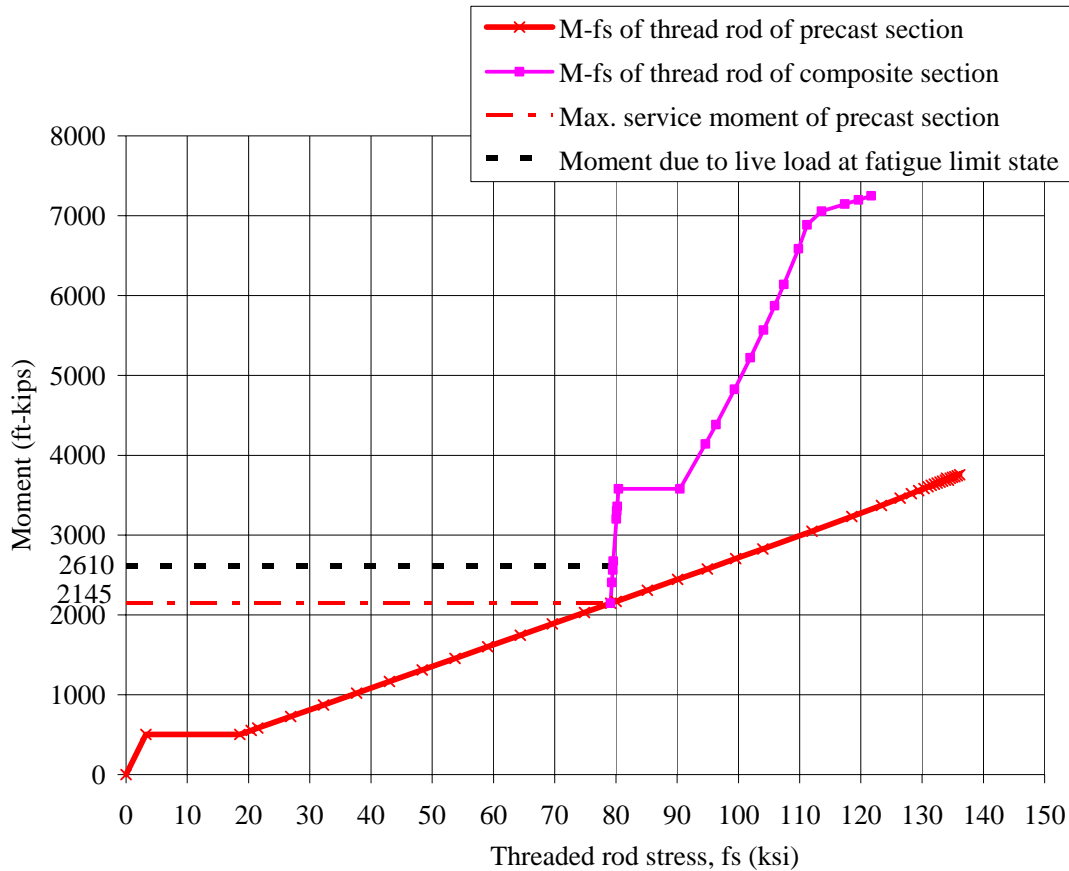
Figure 3.13 Moment-Steel Stress Diagram of Threaded Rod at Fatigue Limit State

Assume the moment due to live load at fatigue limit state is determined as 465 ft-kips. Thus, the stress range of threaded rod is considered at the moment of 2610 ft-kips (2610 ft-kips = 2145 ft-kips + 465 ft-kips). Figure 3.13 shows that the stress range of threaded rod due to the fatigue limit state loading is less than 1 ksi. Even if the deck concrete in tension before cracking is ignored, the rod stress range would be about 5 ksi, which indicates the fatigue limit requirement can be met.

38

3.2 SYSTEM ANALYSIS AT ULTIMATE LIMIT STATE

3.2.1 Flexural Design

The flexural strength of the negative moment section at the ultimate limit state is analyzed based on the strain compatibility and force equilibrium. Two critical sections are suggested for ultimate strength check. They are located at the diaphragm face and the strand transfer length section. The negative moment reinforcement is generally determined based on the loading at the diaphragm face. The transfer length section needs to be considered due to the existence of strands, which might result in a very high neutral axis into the girder thin web and therefore reduce the flexural capacity. This problem can be solved by increasing the concrete strength or adding compression steel to the girder bottom flange. Two loading cases need to be included in the analysis: one is on the precast section immediately after the deck concrete placement, and the other is on the composite section under all the loads.

3.2.2 Shear Design

Because a longer bridge span and/or a wider girder spacing can be achieved by the threaded rod continuity system, shear design is more critical than that of the conventional system, especially at the negative moment zone. It is recommended the AASHTO LRFD Specifications should be adopted for shear design. Using the AASHTO Standard Specifications, however, may result in some invalidity. For instance, the limit of nominal

shear strength by web reinforcement presented as $V_s = 8\sqrt{f_c'} b_w d$ sometimes may make the design unfeasible.

The AASHTO Standard Specifications specify that members subject to shear shall be designed based on $V_u \leq \phi(V_c + V_s)$, where V_u = factored shear force at the section considered, ϕ = strength reduction factor for shear, V_c = nominal shear strength provided by concrete, and V_s = nominal shear strength provided by web reinforcement. The concrete contribution V_c to the shear resistance is taken as the lesser of the inclined cracking strength, V_{ci}, or web cracking strength, V_{cw}, shown as:

$$V_{ci} = 0.6\sqrt{f_c'} b_w d + V_d + \frac{V_i M_{cr}}{M_{max}}$$

$$V_{cw} = (3.5\sqrt{f_c'} + 0.3 f_{pc}) b_w d + V_p$$

where: f_c' = 28-day cylinder compressive strength of concrete; b_w = width of the web; d = effective depth; V_d = shear force at section due to unfactored dead load; V_i = factored shear force at section due to externally applied loads occurring simultaneously with M_{max}; M_{max} = maximum factored moment at section due to externally applied loads; V_p = vertical component of effective prestress force at section; and f_{pc} = compressive stress in concrete (after allowance for prestress losses) at section of cross section resisting externally applied loads. M_{cr} is based on $M_{cr} = \frac{I}{Y_t}(6\sqrt{f_c'} + f_{pe} - f_d)$, in which I = moment of inertia of gross concrete section about the centroidal axis; Y_t = distance from centroidal axis of gross section to extreme fiber in tension; f_d = stress due to unfactored dead load, at extreme fiber of section where tensile stress is caused by externally applied

loads; and f_{pe} = compressive stress in concrete due to effective prestress force only (after allowance for all prestress losses) at the extreme fiber of the section where tensile stress is caused by externally applied load. The value of f_{pe} is considered to be zero at the negative moment zone since the prestress has little effect on the deck slab. Thus,

$M_{cr} = \dfrac{I}{Y_t}(6\sqrt{f_c'} - f_d) = \dfrac{I}{Y_t}(f_r - f_d)$. With a larger span capacity by the threaded rod

continuity system, f_d due to the superimposed dead load becomes higher in comparison with the conventional system. Thus, a lower M_{cr} is obtained, resulting in a lower V_{ci} value, which indicates the shear design for the proposed continuity system is more critical than that of the conventional system.

In the formula accounting for V_{cw}, the item f_{pc} could be negative under some conditions, which results in a very small value of V_{cw} and possibly a small value for V_c. Accordingly, the shear reinforcement contribution, V_s, might exceed the maximum limit of $8\sqrt{f_c'}b_w d$ (f_c' in psi) allowed in the Standard Specifications. In such cases, the compressive strength of concrete has to be increased or a new design has to be undertaken. However, recent experiments show that the limit of $8\sqrt{f_c'}b_w d$ is too conservative. Also, some test results show the proportionate increase in shear strength caused by the increase in shear reinforcement, which either corresponds to or exceeds the maximum reinforcement allowed in the Standard Specifications. It has been confirmed that the LRFD limit of $V_n = \dfrac{V_u}{\phi} \leq 0.25 f_c' b_w d$ is more realistic.

CHAPTER 4

SYSTEM IMPLEMENTATION

4.1 INTRODUCTION

Three bridges in Nebraska have been involved in the implementation of the threaded rod continuity system. They are Pflug Road Bridge (119 ft +119 ft), Clarks Viaduct (100 ft +151 ft +148 ft +128.5 ft), and Wood River Bridge (145 ft + 145 ft).

Pflug Road Bridge in Sarpy County, Nebraska is the first bridge designed with this new technique. Its design started in early 2001. Although the design plans had been completed, the bridge was not constructed. Sarpy County requested that the bridge be pulled out of bidding as the location was desired to be converted to an interchange rather than just an overpass. However, the Pflug Road Bridge provided NDOR designers and UNL researchers with a valuable design and cost assessment experience.

Clarks Viaduct in Merrick County, Nebraska, is the first bridge built in the United States implementing the threaded rod continuity system. It was originally designed as a haunched steel plate girder bridge and let for bid, with the construction contract awarded to Hawkins Construction Company of Omaha, Nebraska. After the construction drawings were released, Tadros Associates, LLC, did the value engineering for this bridge and ended up with a unique concrete alternate incorporating the threaded rod continuity system. The proposed change would guarantee no increase in the superstructure depth, no change in the geometry that included a very difficult 55 degree skew, and no delay in

construction. Furthermore, the new design results in considerable cost savings and a better overall structure.

Wood River Bridge is a two-span bridge, 145 ft +145 ft, which also incorporates the proposed continuity system. The design of this bridge started in May 2003. Its completion is expected to be another successful example of precast concrete bridge design and construction with the threaded rod continuity system.

4.2 PFLUG ROAD BRIDGE

The overall width of Pflug Road Bridge (119 ft +119 ft) is 30.33 ft and the girder spacing is 11 ft. The loading is assumed including the 7.5 in. CIP deck slab weight, barrier weight of 0.382 kips/ft per bridge side, 1.5 in.-thick wearing surface, and traffic load of AASHTO HS-25.

To investigate the advantages using the proposed continuity system, a design comparison is made for an interior girder with the conventional system (see Table 4.1). A standard NU 1100 I-girder section is used for both systems. Note that three girder lines at 11 ft spacing by the conventional system cannot make the design feasible. Instead, four girder lines are required with 46-0.6 in. diameter, Grade 270 strands per girder. With the proposed system, three girder lines at 11 ft. spacing with 44 strands per girder can meet the design requirements. Also shown in Table 4.1 is the required concrete strength for both systems, which is the same due to the different girder spacing considered in this case. With the same bridge span and girder spacing, using the continuity system generally results in reduced demand for concrete strength at release since less prestress is required

in comparison with the conventional system. As a result, it avoids delay in the prestressing bed turnover and reduces the significant financial burden to the precast concrete producer.

A cost analysis shows that approximately $33,000 could be saved for this bridge due to the reduced concrete girder lines in comparison with the conventional system (see Table 4.2). The Pflug Road Bridge implementation project demonstrated that the added cost of the threaded rods and connection hardware was smaller than the savings in positive moment prestressing.

Table 4.1 Design Comparison between the Conventional and Proposed System

	Conventional system	Proposed system
Number of girder lines with NU1100 I-Girder	4	3
f'_{ci} (ksi)	7	7
f'_c (ksi)	9	9
Number of 0.6 in. diameter, Grade 270 strands (per girder)	46	46
Number of 1 3/8 in. diameter, Grade 150 threaded rods (per girder)	0	4

Table 4.2 Cost Comparison between the Conventional and Proposed System

	Conventional system (4 girder lines)	Proposed system (3 girder lines)	Total savings
Savings in concrete girders	0	-$30,012	
Savings in pretensioned strands	0	-$9,235	
Cost of connection hardware and threaded rods	0	$5,671	-$33,576

4.3 CLARKS VIADUCT

Clarks Viaduct presented another opportunity for field demonstration of this new technology. The bridge was originally designed as a steel plate girder bridge. Due to clearance limitations, the girder web depth had to be limited to 48 in. at the positive moment zone, haunched to 72 in. at the piers. The contractor for the project, Hawkins Construction, presented a value engineering proposal to the state involving a number of modifications. One of the modifications was to replace the plate girders with threaded rod spliced precast concrete girders. With the cast-in-place haunches over piers and the special threaded rod continuity for deck weight, an unprecedented span-to-depth ratio of 36 was achieved.

4.3.1 DESIGN OF CLARKS VIADUCT

The Clarks Viaduct was designed based on the following assumptions:

1) The design is based on the AASHTO LRFD Bridge Design Specifications.
2) A 7.5 in. deck weight plus 2 in. girder shim is assumed as 1.110 k/ft per girder line. Barrier weight and wearing surface weight are considered as 0.191 kips/ft and 0.202 kips/ft per girder line, respectively. Live load is HL-93.
3) Deck concrete strength at 28 days, $f_c^{'}$, is 4000 psi.
4) Transformed section properties are used in all service load calculations. Deck thickness is 7 in. for resistance. Girder shim is not included in the section properties.
5) The approximate prestress loss method in NCHRP 18-07 (2002) was used.
6) There is no moment transfer between the superstructure and pier in the superstructure design.
7) The distance between the centerline of bearing and girder end is 1 ft for all precast girders.

The original design consisted of four lines of varying depth plate girders. The depth of plate girder at midspan was about 51 in. and the maximum depth of the haunched plate girder section over piers was approximately 75 in. (see Figure 4.1). A 50 in. deep concrete girder, as shown in Figure 4.2, was modified from the standard NU 1100 I-girder section to match the minimum steel section. The proposed girder section was a standard NU 1100 with one foot of the top flange removed on both sides and 6.7 in. added to the top of the girder. Note that the girder top flange was narrowed in order to save weight. Figure 4.3 illustrates the proposed design versus the original girder profile over the pier, which indicates no increase in the superstructure depth and no change in the geometry. The bridge elevation and the details over the pier are shown in Figure 4.4. After the girders were erected on the CIP pier haunch, they were coupled by the bolted connection detail. A "continuity block" was then cast over the entire area of the pier haunch up to the top of the girders. Section I-I in Figure 4.4 illustrates a composite section made up with the continuity block and the pier haunch. Once the continuity block achieved its required 28-day compressive strength, the deck concrete was poured. Also shown in Figure 4.4 are the critical sections of various spans which were considered in the analysis.

The various loading stages were considered in the analysis. Figure 4.5 lists the moment and shear diagrams due to the different stages of loading. Before the continuity block concrete hardened, the pier haunch had to resist the weight of girder and the wet concrete from the continuity block. Once the continuity block concrete hardened and acted compositely with the pier haunch, the girders were thus made continuous due to

deck weight. After the deck concrete was poured and hardened, the composite section made from the pier haunch, continuity block, and the deck slab resisted the negative moments from the deck weight, superimposed dead load and live load.

Table 4.3 gives the moment and shear at the critical sections of various spans. In the analysis, positive moment sections 1, 5, 9, and 13 were considered to determine the required prestress stress and check the ultimate flexural strength. The required pretensioned strands at various spans are given in Tables 4.4 and 4.5, which also include the required concrete strength at service and release, the required debonded or draped strands, and their corresponding locations. Note that the data shown in Tables 4.4 and 4.5 is based on the independent design by the authors. A more conservative design was adopted in the final plan. Negative moment zones were designed to satisfy the loading due to deck weight plus operation loading for the precast section and that due to all loads for the composite section. Due to the huge negative moment, a cast-in-place pier haunch was incorporated as shown in Figure 4.4. The pier haunch was also designed to provide enough horizontal shear capacity. The cutoff locations of deck reinforcement at the negative moment zone were determined to satisfy the required ultimate flexural strength.
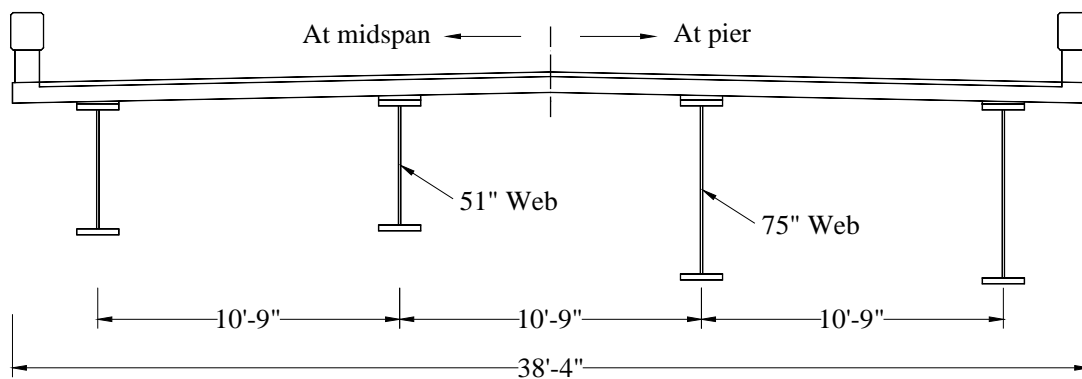
Figure 4.1 Original Steel Bridge Cross Section
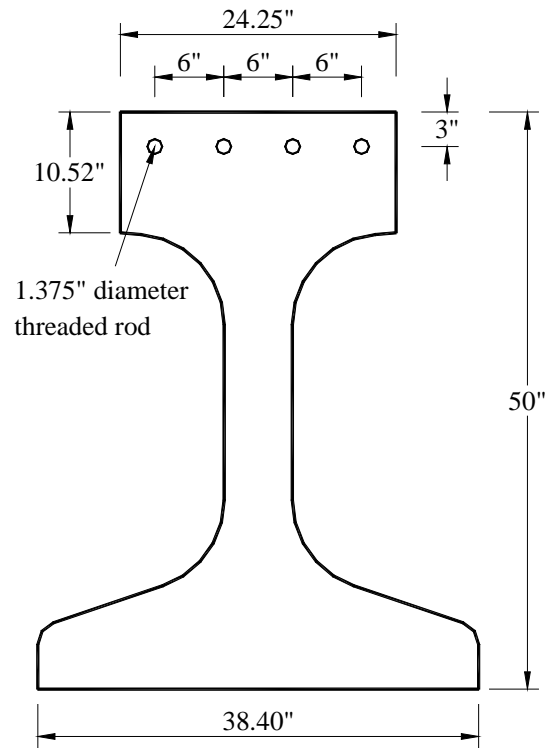
Figure 4.2 Modified NU 1100 I-section
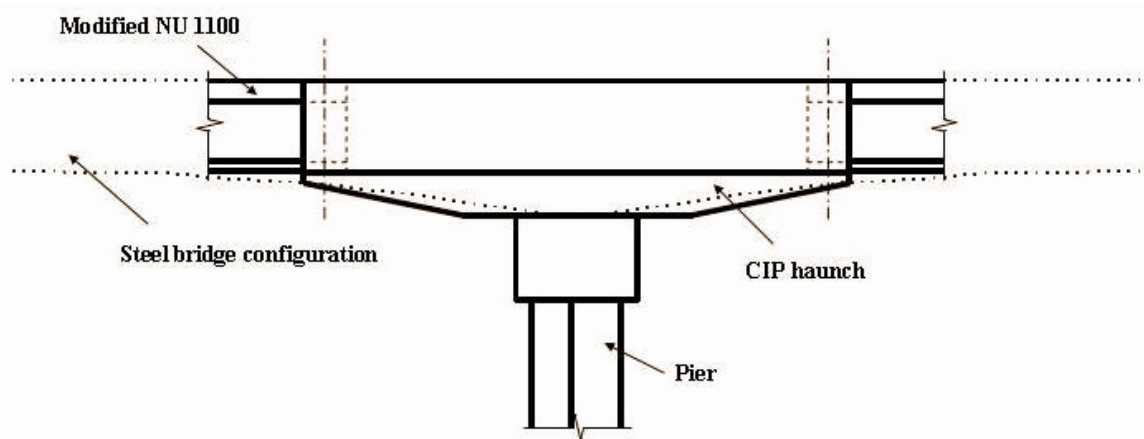
Figure 4.3 Proposed Design versus the Original Bridge Profile over Pier
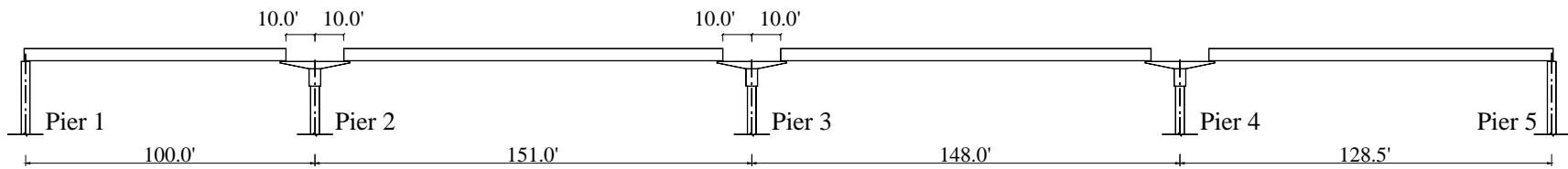
ELEVATION AFTER GIRDER ERECTION

10.0' 10.0'   10.0' 10.0'

Pier 1   Pier 2   Pier 3   Pier 4   Pier 5

100.0'   151.0'   148.0'   128.5'
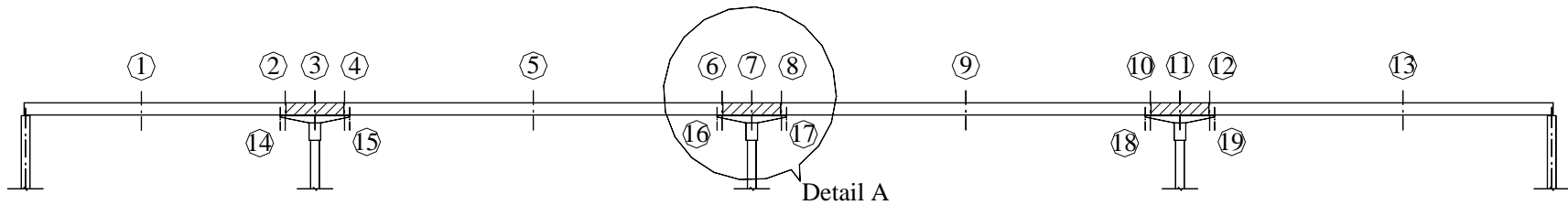
ELEVATION AFTER PLACEMENT OF CONTINUITY BLOCK

Detail A

DETAIL A

10.0'   10.0'   1.0'

Continuity Block   Threaded rod

0.5'

2.0'   2.0'   0.5'
                            Pier haunch
10.0'   4.0'   10.0'

Section I-I

Threaded rod

Continuity block   50"

Roughened surface   9.6'

48"
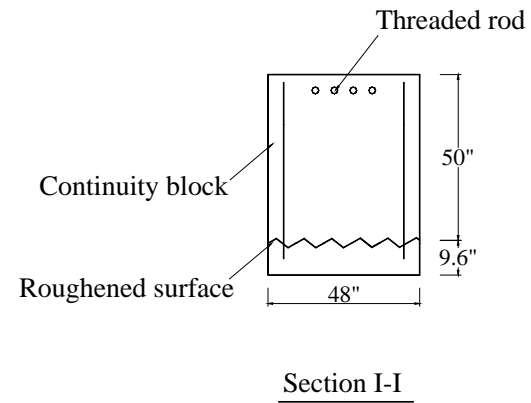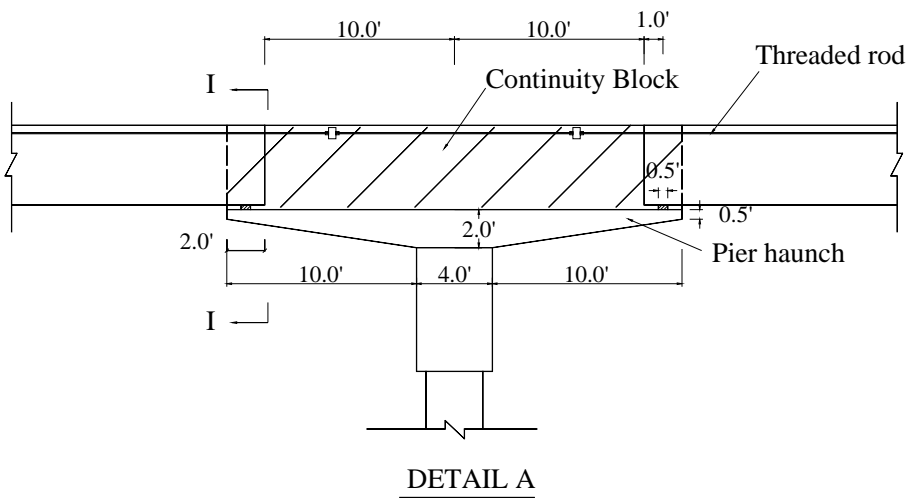
Figure 4.4 Clarks Viaduct Elevation and Details over Pier

| 100.0' | 151.0' | 148.0' | 128.5' |

Loading Stages:

1. Girder erection

2. Continuity block placement

3. Deck placement

4. Barrier

5. Wearing surface

6. LL+IM

Figure 4.5 Moment and Shear Diagrams at Various Loading Stages

50

Table 4.3 Moment and Shear at Various Critical Sections

Bending Moment (Load factor = 1.0)   Per Interior Girder*

Note: Assume girder spacing = 10.75 ft.

Section No.	Section Designation	Moment (kips-ft)						
		Girder+Haunch	Continuity block	Deck	Barrier	Wearing surface	M_{LL+IM} (Max)	M_{LL+IM} (Min)
1	0.400	805.6	0.0	538.1	94.3	99.7	1944.0	
2	0.890	-0.8	0.0	-1382.6	-233.0	-246.4		-2192.0
3	1.000	-417.0	-125.6	-2091.4	-354.4	-374.8		-2862.0
4	1.073	-0.8	0.0	-1320.9	-222.0	-234.8		-1738.0
5	1.500	1710.0	0.0	980.8	172.8	182.8	2150.0	
6	1.927	-0.8	0.0	-1479.6	-251.8	-266.3		-1989.0
7	2.000	-417.0	-125.6	-2274.3	-388.7	-411.1		-2771.0
8	2.074	-0.8	0.0	-1518.5	-258.4	-273.3		-1984.0
9	2.500	1631.0	0.0	690.1	123.0	130.1	2161.0	
10	2.926	-0.8	0.0	-1584.0	-267.0	-282.4		-1925.0
11	3.000	-417.0	-125.6	-2423.8	-411.1	-434.8		-2856.0
12	3.086	-0.8	0.0	-1577.3	-266.0	-281.3		-1979.0
13	3.600	1396.4	0.0	1238.6	215.3	227.7	2461.0	

Shear (Load factor = 1.0)   Per Interior Girder

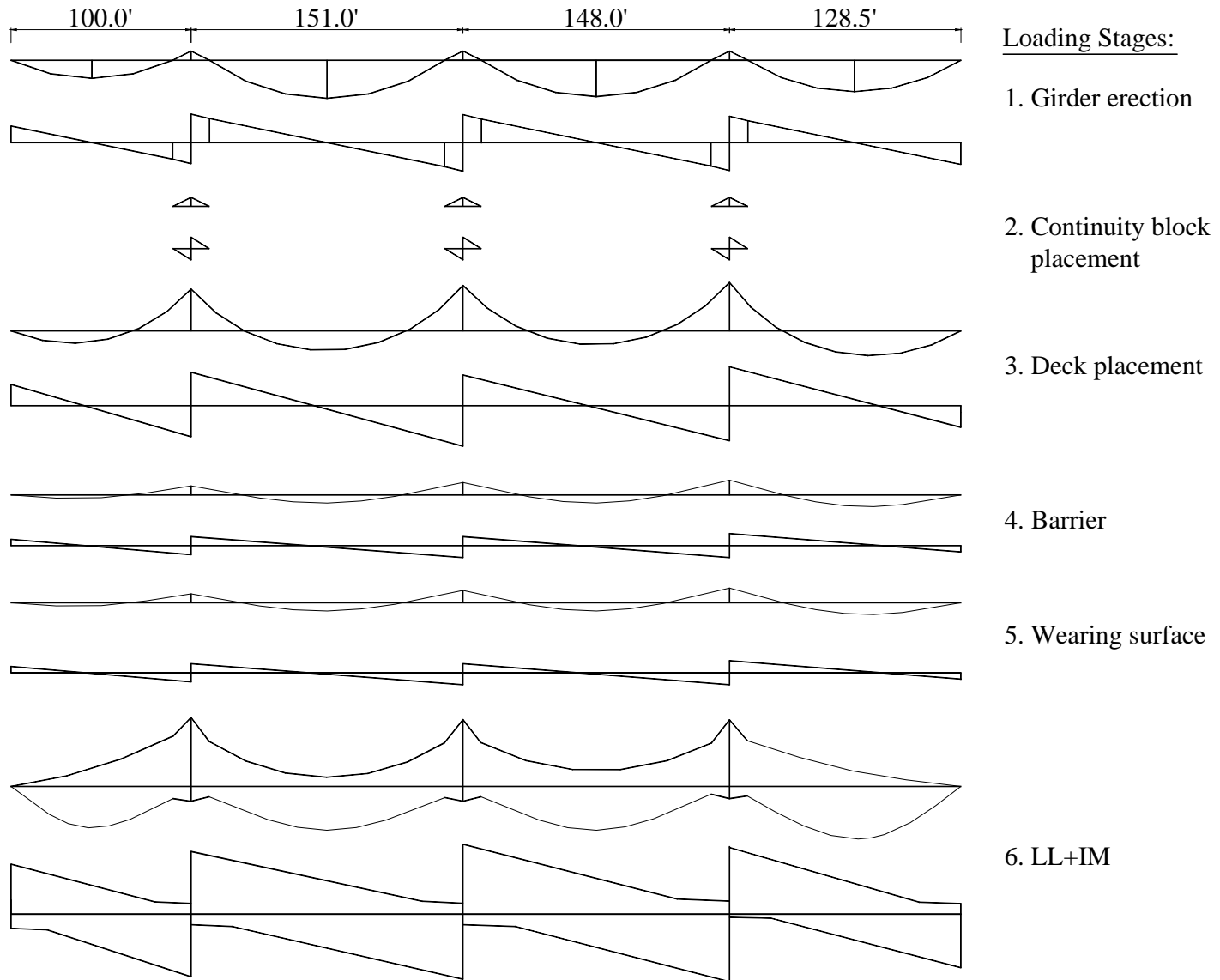| Section No.	Section Designation	Shear (kips)						
		Girder+Haunch	Continuity block	Deck	Barrier	Wearing surface	V_{LL+IM} (Max)	V_{LL+IM} (Min)
1	0.400	3.7	0.0	-15.3	-1.6	-1.7	52.0	-53.9
2	0.890	-36.6	0.0	-65.3	-11.2	-11.8		-145.0
3	1.000 (Left)	-46.6	-25.1	-76.4	-13.0	-13.7		-146.7
	1.000 (Right)	63.0	25.1	82.6	14.2	15.0	152.3	
4	1.073	53.0	0.0	71.5	12.3	13.0	138.0	
5	1.500	0.0	0.0	-1.2	-0.2	-0.2	59.8	-58.0
6	1.927	-53.0	0.0	-73.9	-12.7	-13.4		-138.0
7	2.000 (Left)	-63.0	-25.1	-85.0	-14.6	-15.4		-156.6
	2.000 (Right)	61.8	25.1	81.1	14.0	14.8	154.4	
8	2.074	51.8	0.0	70.0	12.1	12.8	137.0	
9	2.500	0.0	0.0	-1.0	-0.2	-0.2	60.0	-60.0
10	2.926	-51.8	0.0	-72.0	-12.4	-13.1		-137.0
11	3.000 (Left)	-61.8	-25.1	-83.1	-14.3	-15.1		-150.9
	3.000 (Right)	58.3	25.1	90.1	15.5	16.4	155.6	
12	3.086	48.3	0.0	79.0	13.6	14.4	137.0	
13	3.600	-6.0	0.0	6.0	1.0	1.1	55.8	-54.0

Table 4.4 Design based on Prestress at Service

Span (ft)	Number of 0.6" strands	Concrete bottom stress at critical positive section at final (ksi)
100	22	-0.15
151	40	-0.06
148	40	0.37
128.5	40	-0.25

Note: Tensile stress is negative.

Table 4.5 Design based on Prestress at Release

Span (ft)	f'_{ci} (ksi)	Max. concrete stress at release (ksi)		Amount and location (from girder end) of draped and debonded strands
		Bottom fiber	Top fiber	
100	5.7	2.19	-0.07	4 draped strands at 36.4 ft (0.4 of girder length); no debonded strands.
151	5.7	3.30	-0.10	4 draped strands at 52.4 ft (0.4 of girder length); 10 debonded at 26.2 ft (0.2 of girder length).
148	5.7	3.34	-0.11	4 draped strands at 51.2 ft; 10 debonded at 25.6 ft.
128.5	5.7	3.39	0.08	6 draped strands at 47.8 ft; 10 debonded at 23.9 ft.

4.3.2 CONSTRUCTION OF CLARKS VIADUCT

The construction procedures of Clarks Viaduct are described as follows: 1) install the pier and abutment; 2) cast the pier haunch; 3) erect and align the precast girder; 4) couple the girders using the bolted connection detail; 5) cast the continuity block; 6) cast the deck slab; and 7) install the barriers and complete the bridge construction.

As shown in Figure 4.6, each pier consisted of four columns on individual piles supported footings and a pier cap. The pier columns were centered directly under each girder line. The CIP haunch blocks were created over the top of the pier cap. Concrete with a 28-day strength of 5,000 psi was used. Figure 4.7 shows the modified NU 1100 I-section girders in the precast yard.

Note that 4-1 3/8 in. diameter, Grade 150 ksi threaded rods located at the girder top flange and projected outside of the girder ends. Once the pier haunch gained the required concrete strength, the precast girders were erected and placed as shown in Figure 4.8. A total of 14-#8 bars were used to reinforce the pier haunch during erection based on the loading case given in Figure 4.9. Figure 4.10 is presented to show the girder camber.

The bolted connection detail was incorporated to couple the precast girders (see Figures 4.11, 4.12 and 4.13). The continuity blocks over the pier haunch were cast prior to the placement of the deck slab, as illustrated in Figure 4.14. Figures 4.15 and 4.16 show the deck formation, and the reinforcement setup is presented in Figure 4.17. The bridge deck was poured in April 2003, as illustrated in Figure 4.18. Bridge construction was completed in July 2003 (see Figure 4.19). According to feedback from the contractor, no problems have been encountered in utilizing the threaded rod continuity system during the construction process.

Clarks Viaduct is the first bridge in the United States to implement the proposed continuity system. With the CIP haunches and the special threaded rod continuity for deck weight, a span-to-depth ratio of 36 is achieved. The value engineering of Clarks Viaduct shows this new system can be simply incorporated into the concrete superstructures as an alternative to compete with long span steel bridges. The value engineering also demonstrated the economy of this innovative system. This system will not only result in long-term savings such as lower maintenance costs, but also will provide immediate benefits to the owner and the contractor in construction cost savings. The overall construction savings for Clarks Viaduct were approximately $100,000.

Figure 4.6 Pier Setup and Haunch Block Forming

Figure 4.7 Modified NU 1100 I-section Girder in the Precast Yard

Figure 4.8 Precast Girders during Erection

Figure 4.9 Precast Girders Placed on Pier Haunch

Figure 4.10 View of Precast Girders Placed over Pier Haunch along the Traffic Direction

Figure 4.11 Precast Girder Coupled by Bolted Connection Detail

Figure 4.12 A Closer Look at the Connection Detail over Pier

Figure 4.13 Girders Coupled by Threaded Rods before Continuity Block Placement

Figure 4.14 Concrete Placement of Continuity Block over Pier

Figure 4.15 Side View of Deck Forming

Figure 4.16 View of Deck Forming below the Bridge

Figure 4.17 Deck Reinforcement Setup

Figure 4.18 Casting the Bridge Deck

Figure 4.19 Completion of Bridge Construction

4.3.3 MONITORING OF CLARKS VIADUCT

As one of the most important construction phases, the Clarks Viaduct bridge deck placement was monitored. The stresses of threaded rods and girder deflection at this loading stage were observed. Before the precast girders were shipped to the bridge construction site, eight strain gauges were attached to the threaded rods at various girders, as shown in Figure 4.20. Despite of the protection, only three strain gauges were prevented from being damaged during the girder shipping and deck forming process. Two gauges were located at approximately section 8 and section 6 (see Figure 4.3 for section locations and Figure 4.21 for gauges in site). Immediately after the deck concrete was poured, the strain readings of the gauges were observed as 1227×10^{-6}, 1114×10^{-6} and 998×10^{-6}, respectively. The stresses of threaded rods due to deck and operation weight were thus computed to be 35.6 ksi, 32.3 ksi, and 28.9 ksi.

Figure 4.20 Strain Gauges Attached to Threaded Rods in the Precast Yard

Figure 4.21 Strain Gauges in the Construction Field

In order to compare the theoretical values with the observed data, the Section I-I in Figure 4.4 was analyzed. The moment-stress diagram of the threaded rod was presented in Figure 4.22. From Table 4.3, the moment due to deck weight at section 6 and section 8 is 1480 kips-ft and 1519 kips-ft, respectively. According to Figure 4.22, the stresses of threaded rods can be determined as 52.6 ksi due to the moment of 1480 kips-ft and 54.0 ksi due to the moment of 1519 kips-ft, respectively. Thus, it appears there is some discrepancy between the analysis results and observed data.
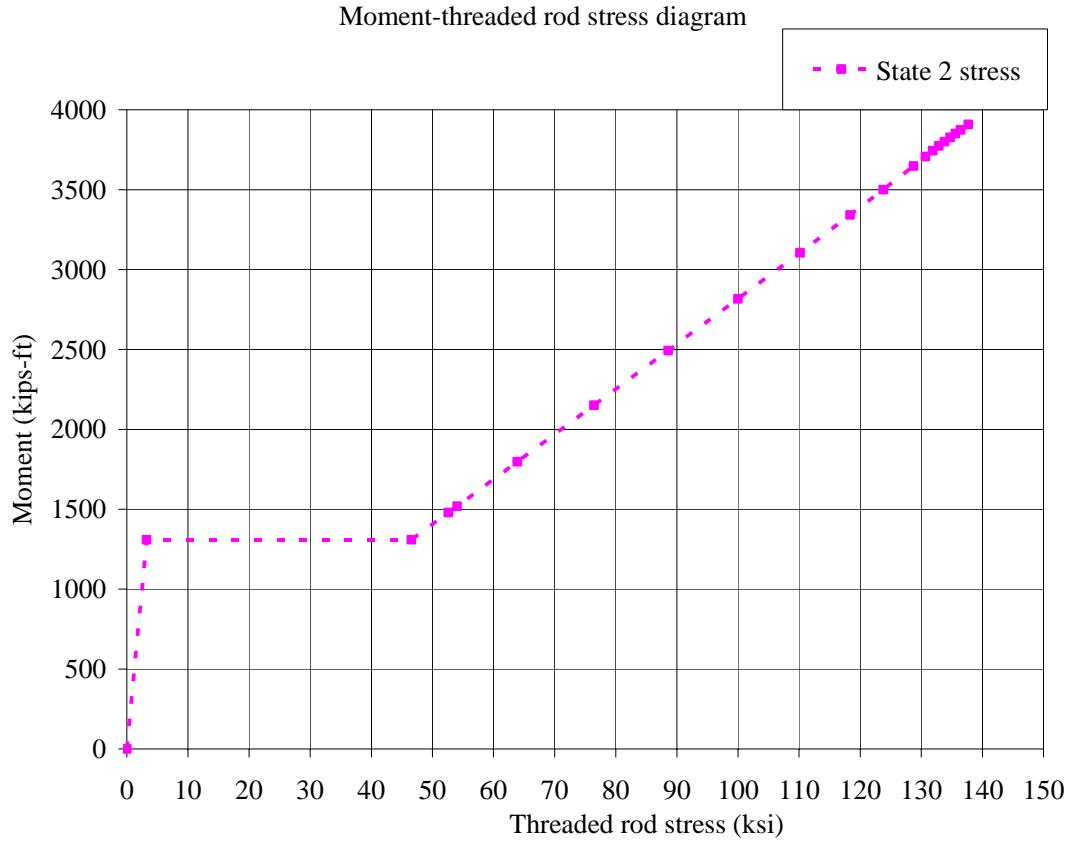
Moment-threaded rod stress diagram

Figure 4.22 Moment-threaded Rod Stress Diagram of the Analyzed Section

Note that the given section over pier is analyzed to be cracked under the moment due to deck weight. For a bending moment $M > M_{cr}$, cracking occurs and the steel stress along the reinforcement varies from a maximum value at the crack location to a minimum value at the middle of the spacing between the cracks. Based on the formula given by Ghali (2002), a mean value of steel strain can be obtained, which is expressed by $\varepsilon_{sm} = (1 - \zeta)\varepsilon_{s1} + \zeta\varepsilon_{s2}$. ε_{sm} represents an overall mean strain value for the cracked member; ε_{s1} is a hypothetical strain in the reinforcement assuming state 1 (a section just before cracking) continues to apply when $M > M_{cr}$; ε_{s2} is the steel strain at state 2 which refers to the cracked section. $\zeta = 1 - \beta_1\beta_2\left(\dfrac{M_{cr}}{M}\right)^2$, and it is a dimensionless coefficient, between 0 and 1, representing the

63

extent of cracking. $\zeta = 0$ is for an uncracked section and $0 < \zeta \leq 1$ for a cracked section. $\beta_1 = 1.0$ is used for deformed bars, and $\beta_2 = 0.5$ for sustained or cyclic loading.

The mean strain of threaded rod was plotted in Figure 4.23. Accordingly, the mean rod stress can be determined from the power formula given in the PCI Bridge Design Manual. As shown in Figure 4.24, the mean stresses of threaded rod were determined as 33.5 ksi due to the moment of 1480 kips-ft and 35.4 ksi due to the moment of 1519 kips-ft, which is close to the observed data.
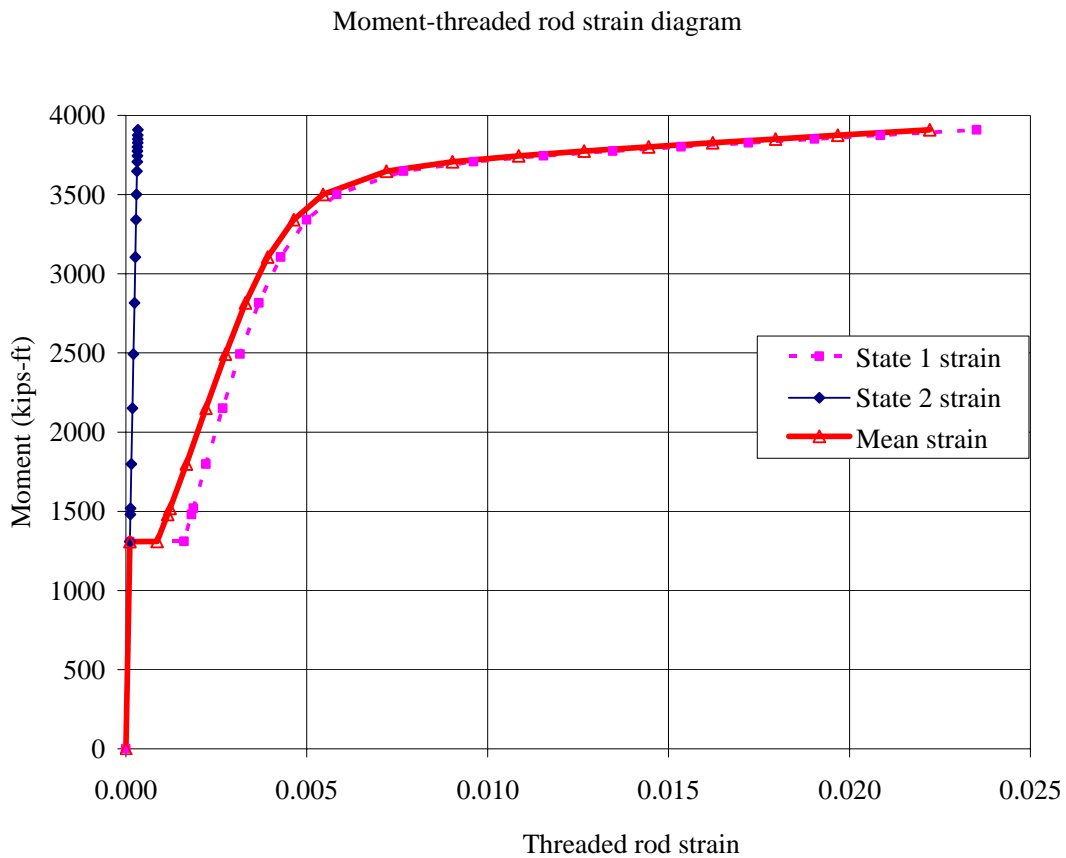
Moment-threaded rod strain diagram

Figure 4.23 Determination of Mean Strain for the Threaded Rod
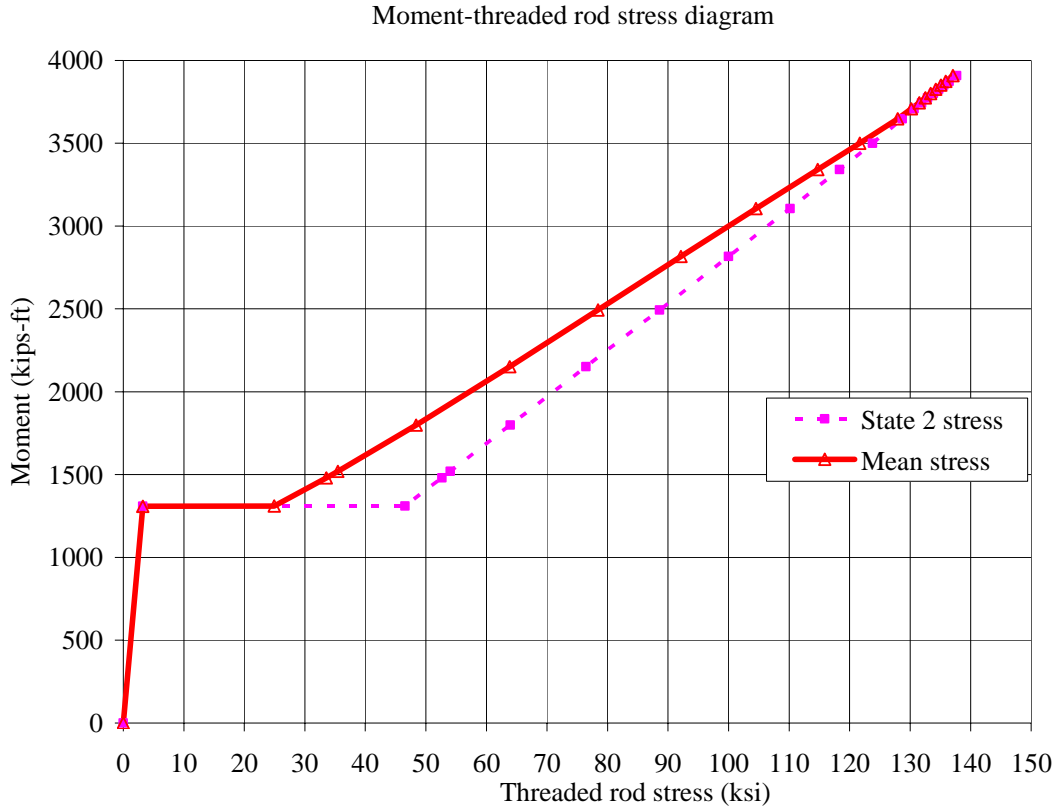
Moment-threaded rod stress diagram

Figure 4.24 Determination of Mean Threaded Rod Stress

The deflection of four girders at span 3 (148 ft span) was observed just after deck placement (see Figure 4.25). Since the highway under the bridge was not blocked when the deck concrete was poured, it was too difficult to check the midspan deflection. Eventually, the checking points were located approximately 35 ft away from the centerline of pier 4 (see Figure 4.4). The observed deflection was averaged to be 1.20 in. for the various checking points. Based on the analysis from RISA 2D, where the moment of inertia of cracked section was used in the negative moment zone, the deflection was computed to be 1.32 inch. Thus, the analysis result is close to the observed data.

Figure 4.25 Determination of Girder Deflection

4.4 WOOD RIVER BRIDGE

Wood River Bridge is a two-span bridge, 145 ft +145 ft, where the proposed continuity system was implemented. The girder spacing is 8 ft. A modified NU 1100 I-section, as shown in Figure 4.26, was used by adding 3 in. height to the standard NU 1100 section. Note that five 1 1/2 in. diameter, Grade 150 ksi H. S. threaded rods were embedded in the girder top flange. Five threaded rods instead of four were included herein since the NDOR designers recommended a factor of 1.5 to account for the negative moment due to deck weight. As opposed to Clarks Viaduct, the girder top flange width was not reduced based on the NDOR designers' suggestion, which reflected some contractor's preference to wider girder flange for deck forming. Table 4.6 gives design results for an interior girder.
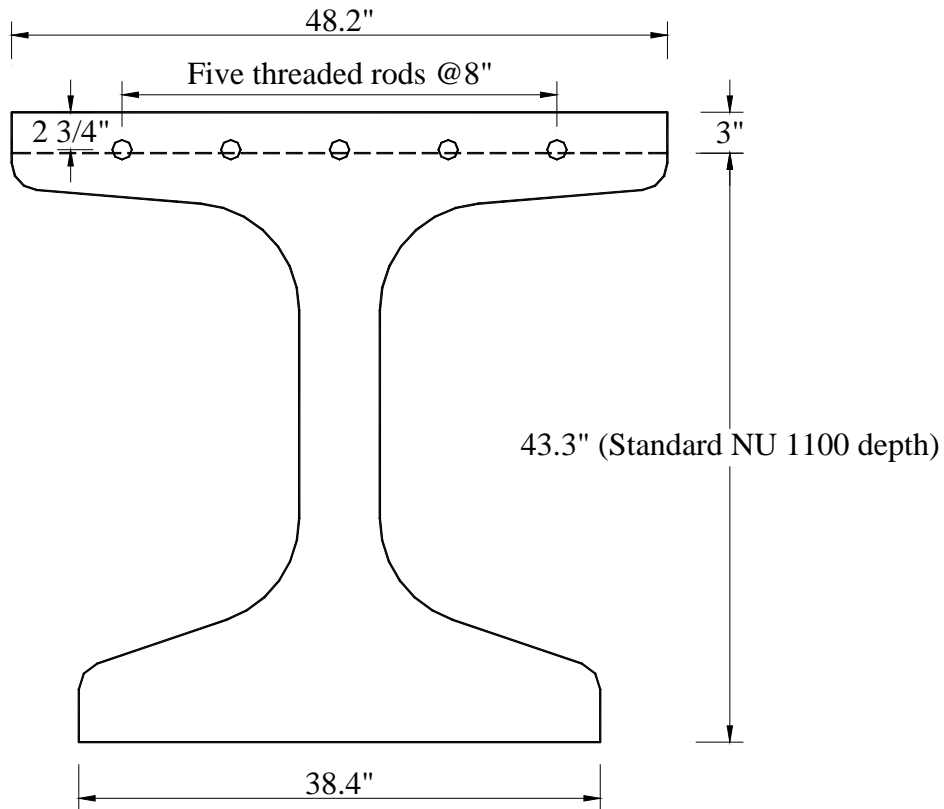
Figure 4.26 Modified NU 1100 I-section for Wood River Bridge

Table 4.6 Wood River Bridge Design

	Positive moment section at 0.4span	Negative moment section at face of diaphragm
$f_c^'$ (ksi)	11.0	11.0
$f_{ci}^'$ (ksi)	6.5	6.5
No. of 0.6" strands	58	58 (12 draped, 10 debonded)
No. of 1 1/2" Grade 150 ksi threaded rods	0	5
Deck reinf. at the top layer	#5 @12"	3#8 @12"
Deck reinf. at the bottom layer	#5 @12"	(#5 + #8) @12"

CHAPTER 5

CONCLUSIONS

This report presents an innovative threaded rod continuity system that makes precast bridge girders continuous for deck weight. A standard bolted connection detail has been developed to couple the precast girders. A number of significant advantages of the proposed continuity system over the conventional system have been discussed in the report. The conclusions are as follows:

1) Since the precast girders are made continuous for approximately two-thirds of the loads, the positive moment is greatly reduced, resulting in reduced demand for prestress and for high strength concrete at release.

2) The same girder size can span about 15 percent longer than with the conventional system.

3) The bridge performance is improved as the negative moments due to deck weight more than offset the positive moments due to time-dependent restraints without cracking at the piers.

4) The full-scale testing of this system at the University of Nebraska has shown that it can provide full continuity due to deck slab weight with superior structural performance.

5) The threaded rod continuity system is believed to be an efficient solution to make deck weight continuous without post-tensioning. It is simple for construction

without need for a specialty contractor. Implementation of this system in the Clarks Viaduct project in Nebraska shows it can be constructed efficiently.

6) This system provides a feasible alternative for concrete superstructures to compete with long span steel bridges and results in moderate cost savings.

7) The proposed connection detail can be incorporated into other types of girders such as inverted tee beams and box beams.

8) A simple Excel spreadsheet can be easily developed as a design tool. Currently, commercial software cannot be used to design the precast girders made continuous for deck weight. However, CONSPAN and PSBeam are working on modifying their software to adopt this new concept.

REFERENCES

- AASHTO, LRFD Bridge Design Specifications, Second Edition 1998 and Interims 1999 and 2000, American Association for State Highway and Transportation Officials, Washington, D.C.

- AASHTO, Standard Specifications for Highway Bridges, 16th Edition, American Association for State Highway and Transportation Officials, Washington, D.C., 1996.

- Abdel-Karim, A., and Tadros, M. K, "State-of-the-Art of Precast/Prestressed Concrete Spliced-Girder Bridges", PCI Special Publication, Precast/Prestressed Concrete Institute, Chicago, IL, October 1992.

- Branson, D.E., "Deformation of Concrete Structures", McGraw-Hill, New York, 1977.

- Destefano, Ralph, Evans, Jack, Sun, Chuanbing and Tadros, Maher K., "Flexural Crack Control in Concrete Bridge Structures", Proceedings of the 2003 High Performance Concrete Symposium and Bridge Conference, October 2003.

- Girgis, Amgad, Sun, Chuanbing, and Tadros, Maher K., "Problems and Solutions – Flexural Strength of Continuous Bridge Girders – Avoiding the Penalty in the AASHTO LRFD Specifications, PCI Journal Vol. 47, no.4, p 138-141, July-August 2002

- Hennessey, Shane A., Bexten, Karen, Sun, Chuanbing, and Tadros, Maher K., "Value Engineering of Clarks Viaduct in Nebraska", Proceedings of 2002 High Performance Concrete Symposium and Bridge Conference, October 2002

- Ma, Zhongguo (John), Huo, Xiaoming, Tadros, Maher K. and Baishya, Mantu, "Restrained Moments in Precast/Prestressed Concrete Continuous Bridges", PCI JOURNAL, V. 43, No. 6, November-December 1998, pp. 40-57.

- Mirmiran, A., Kulkarni, S., Castrodale, R., Miller, R., and Hastak, M., "Nonlinear Continuity Analysis of Precast, Prestressed Concrete Girders with Cast-in-Place Decks and Diaphragms," PCI JOURNAL, Vol. 46, No. 5, September-October 2001, pp. 60-80.

- Oesterle, R. G., Glikin, J. D. and Larson, S. C., "Design of Precast Prestressed Bridge Girders Made Continuous", NCHRP Report 322, TRB, National Research Council, Washington, D.C., November 1989, pp. 1-5.

- "Precast/Prestressed Concrete Institute Bridge Design Manual (PCI-BDM)", Precast/Prestressed Concrete Institute, Chicago, IL, October 1997

- Sun, Chuanbing, Badie, Sameh S. and Tadros, Maher K., "New Details for Precast Concrete Girders made Continuous for Deck Weight", Proceedings of the TRB 81st Annual Meeting, Washington, DC, Jan. 12-16, 2002

- Tadros, M. K., Ficenec, Joseph A., Einea, Amin, and Holdsworth, Steve, "A New Technique to Create Continuity in Prestressed Concrete Members", PCI JOURNAL, V. 38, No. 5, September-October 1993, pp. 30-37.

- Wasserman, E. P., "Tennessee State Route 50 Bridge over Happy Hollow Creek", PCI JOURNAL, V. 44, No. 5, September-October 1999, pp. 26-40.